
ISSN 0016-7037
Volume 75, Number 1
January 1, 2011

ELSEVIER

Geochimica et Cosmochimica Acta

JOURNAL OF THE GEOCHEMICAL SOCIETY
AND THE METEORITICAL SOCIETY

Volume 75, Number 1 January 1, 2011

Articles

Continued on outside back cover

(This is a sample cover image for this issue. The actual cover is not yet available at this time.)

Available online at www.sciencedirect.com

SciVerse ScienceDirect

Geochimica et Cosmochimica Acta 78 (2012) 99–118

Geochimica et Cosmochimica Acta

www.elsevier.com/locate/gca

Spatial variability of initial $^{230}Th/^{232}Th$ in modern *Porites* from the inshore region of the Great Barrier Reef

Tara R. Clark [a,*], Jian-xin Zhao [a,b], Yue-xing Feng [b], Terry J. Done [c], Stacy Jupiter [d], Janice Lough [c], John M. Pandolfi [e]

[a] *School of Earth Sciences, The University of Queensland, Brisbane QLD 4072, Australia*
[b] *Radiogenic Isotope Laboratory, Centre for Microscopy and Microanalysis, The University of Queensland, Brisbane QLD 4072, Australia*
[c] *Australian Institute of Marine Science, Townsville, Australia*
[d] *Wildlife Conservation Society, Fiji Country Program, Suva, Fiji*
[e] *Centre for Marine Science, School of Biological Science, ARC Centre of Excellence in Coral Reef Studies, The University of Queensland, Brisbane QLD 4072, Australia*

Received 23 February 2011; accepted in revised form 15 November 2011

Abstract

The main limiting factor in obtaining precise and accurate uranium-series (U-series) ages of corals that lived during the last few hundred years is the ability to constrain and correct for initial thorium-230 ($^{230}Th_0$), which is proportionally much higher in younger samples. This is becoming particularly important in palaeoecological research where accurate chronologies, based on the ^{230}Th chronometer, are required to pinpoint changes in coral community structure and the timing of mortality events in recent time (e.g. since European settlement of northern Australia in the 1850s). In this study, thermal ionisation mass spectrometry (TIMS) U-series dating of 43 samples of known ages collected from living *Porites* spp. from the far northern, central and southern inshore regions of the Great Barrier Reef (GBR) was performed to spatially constrain initial $^{230}Th/^{232}Th$ ($^{230}Th/^{232}Th_0$) variability. In these living *Porites* corals, the majority of $^{230}Th/^{232}Th_0$ values fell within error of the conservative bulk Earth $^{230}Th/^{232}Th$ atomic value of $4.3 \pm 4.3 \times 10^{-6}$ (2σ) generally assumed for $^{230}Th_0$ corrections where the primary source is terrestrially derived. However, the results of this study demonstrate that the accuracy of ^{230}Th ages can be further improved by using locally determined $^{230}Th/^{232}Th_0$ values for correction, supporting the conclusion made by Shen et al. (2008) for the Western Pacific. Despite samples being taken from regions adjacent to contrasting levels of land modification, no significant differences were found in $^{230}Th/^{232}Th_0$ between regions exposed to varying levels of sediment during river runoff events. Overall, 39 of the total 43 $^{230}Th/^{232}Th_0$ atomic values measured in samples from inshore reefs across the entire region show a normal distribution ranging from 3.5 ± 1.1 to $8.1 \pm 1.1 \times 10^{-6}$, with a weighted mean of $5.76 \pm 0.34 \times 10^{-6}$ (2σ, MSWD = 8.1). Considering the scatter of the data, the weighted mean value with a more conservative assigned error of 25% (i.e. $5.8 \pm 1.4 \times 10^{-6}$) that encompasses the full variation of the 39 $^{230}Th/^{232}Th_0$ measurements is recommended as a more appropriate value for initial ^{230}Th corrections for U-series dating of most *Porites* samples from inshore regions of the GBR. This will result in significant improvement in both the precision and accuracy of the corrected ^{230}Th ages related to those based on the assumed bulk Earth $^{230}Th/^{232}Th_0$ value of $4.3 \pm 4.3 \times 10^{-6}$. However, several anomalously high $^{230}Th/^{232}Th_0$ values reaching up to $28.0 \pm 1.6 \times 10^{-6}$ occasionally found in some coral annual bands coinciding with El Niño years imply high $^{230}Th/^{232}Th_0$ sources and highlight the complexities of understanding $^{230}Th/^{232}Th_0$ variability. For U-series dating of young coral samples from such sites where anomalous $^{230}Th/^{232}Th_0$ values occur, we suggest replicate dating of multiple growth bands with known age difference to verify age accuracy.

* Corresponding author. Tel.: +61 7 3346 7382; fax: +61 7 3365 8530.
E-mail address: t.clark1@uq.edu.au (T.R. Clark).

0016-7037/$ - see front matter © 2011 Elsevier Ltd. All rights reserved.
doi:10.1016/j.gca.2011.11.032

1. INTRODUCTION

Palaeo-environmental research has become increasingly important in understanding present as well as past marine ecosystem dynamics, as long-term sustained ocean observations are limited in space and time. In particular, understanding the effects of current climate change and anthropogenic disturbance on coral reefs is highly topical as coral reefs worldwide become seriously degraded or begin to show signs of decline (Pandolfi et al., 2003). Both modern and fossil coral skeletons have proven to contain valuable proxies for reconstructing past climate (e.g. Gagan et al., 2000; Cobb et al., 2003a), sea level (e.g. Chen et al., 1991; Chappell et al., 1996) and water quality (e.g. McCulloch et al., 2003; Lewis et al., 2007). They also temporally constrain a broad range of physical processes including the timing of tectonic and seismic activity (e.g. Edwards et al., 1988; Zachariasen et al., 1999; Natawidjaja et al., 2004; Sieh et al., 2008), storm events (e.g. Zhao et al., 2009a; Yu et al., 2009), and other major environmental disturbances (e.g. Abram et al., 2003; Yu et al., 2006). However, as this field of research continues to grow, so does the need to place these studies in an accurate chronological framework.

Uranium-series (U-series) or uranium–thorium (U/Th) isotopic dating is a well established technique that provides an ideal method for determining the age of carbonates over a time range from a few years (e.g. Edwards et al., 1988; Yu et al., 2006; Shen et al., 2008) up to 600 thousand years (ka) (e.g. Stirling et al., 2001) using mass spectrometry. This is based on the principle that uranium is relatively soluble in oxidised waters and taken up by the coral during skeletogenesis. Thorium on the other hand, is relatively insoluble in oxidised waters and minute in the aragonite skeleton of surface water corals. Provided that the system remains closed to the addition or removal of uranium and thorium and the precipitate is free from thorium contamination, the age of the coral can be determined by measuring the ratio of the daughter ^{230}Th and intermediate daughter ^{234}U nuclide to its parent, ^{238}U.

However, less attention has been paid to dating young corals from coastal environments which receive substantial terrestrial input in the form of silts and clays from nearby rivers with a significant amount of adsorbed extraneous ^{230}Th. The reasons for this are reviewed in detail by Zhao et al. (2009b). In summary, the abundance of total ^{230}Th is significantly lower in young carbonates, resulting in the low ^{230}Th signal being complicated by contributions from procedural blanks, instrumental baselines and contamination during analysis. Moreover, the presence of higher proportions of $^{230}Th_0$ can result in substantial uncertainties associated with age corrections compared to material of greater age. With the recent advancement of the U-series dating technique, the former is less of a concern as analytical uncertainties have become significantly reduced with recent developments in thermal ionisation mass spectrometry (TIMS) and multi-collector inductively coupled plasma mass spectrometry (MC-ICPMS) with typical 2-sigma age error of ±1–2 years or less for samples with uncorrected ^{230}Th dates <100 years readily achievable (see Zhao et al., 2009b for review). The latter, however, can render a precise U-series date meaningless if $^{230}Th_0$ is proportionally too high and no effort is made to constrain the range of possible initial $^{230}Th/^{232}Th$ ($^{230}Th/^{232}Th_0$) values.

While most shallow-water corals with high detrital thorium levels or Th/U ratios can be generally avoided, in some instances, dating such corals is necessary where the availability of good-quality, pristine samples are limited (e.g. Lybolt et al., 2010). Fortunately, there are several methods to either remove or correct for allochtonous ^{230}Th. By adopting a vigorous cleaning procedure, the bulk of the $^{230}Th_0$ fraction usually bound to detrital particles trapped in the carbonate matrix can be effectively removed (Stein et al., 1991). Isochrons for a series of coeval samples of the same deposit with variable Th/U ratios are also used to accurately determine both the age and $^{230}Th/^{232}Th_0$ value of the deposit (Bischoff and Fitzpatrick, 1991; Shen et al., 2008). In addition, site specific $^{230}Th/^{232}Th_0$ values can also be calculated from U-series measurements of corals with ages being independently determined through band counting or geochemical proxy wiggle-matching (Cobb et al., 2003b; Yu et al., 2006; McCulloch and Mortimer, 2008; Shen et al., 2008). The mean value of these site-specific $^{230}Th/^{232}Th_0$ measurements can then be applied to determine ages of other dated corals from the same site.

Commonly, assumptions are made on the source of the $^{230}Th_0$ component present in carbonate material; usually clays of terrestrial origin. In the past, the terrestrial upper continental or bulk Earth value has been routinely assigned to U-series age equations to correct for $^{230}Th_0$ (e.g. Stein et al., 1991; Eisenhauer et al., 1993). This value is based on the Th/U ratio of silicates in the upper continental crust, which has a range of 3.6–3.8 (Taylor and McLennan, 1995; Wedepohl, 1995). Assuming secular equilibrium between ^{230}Th and ^{238}U, this would give an atomic ratio (used hereafter) of $4.48–4.70 \times 10^{-6}$ (Richards and Dorale, 2003). A more conservative value of $4.3 \pm 4.3 \times 10^{-6}$ (2σ) includes the full range of Th/U values (Richards and Dorale, 2003), and has proven sufficient for dating most fossil corals with moderate precision (Shen et al., 2008). However, it is now well known that anomalous values of $^{230}Th/^{232}Th_0$ can be inherited in some environments where sources of $^{230}Th_0$ include wind blown aeolian dust (as low as $\sim 1.46 \times 10^{-6}$), dissolved and particulate thorium in open-ocean seawater ($\sim 5–10 \times 10^{-6}$), seawater from upwelling areas ($\sim 2 \times 10^{-4}$), and carbonate sands (up to $\sim 1 \times 10^{-2}$) (Cobb et al., 2003b; Robinson et al., 2004; Shen et al., 2008).

Consequently, there is a large disparity in initial ^{230}Th in corals sampled over broad spatial scales (Table 1), signifying the need for specific correction values to be applied to samples at sites where $^{230}Th/^{232}Th_0$ variability is high in order to improve the accuracy and precision of coral ages obtained using U-series methods to a precision of ±1 years for modern corals (Shen et al., 2008). Simply correcting U-series ages of corals with the bulk Earth $^{230}Th/^{232}Th_0$ value may result in age bias (Shen et al., 2008; Zhao et al., 2009b).

Considering the need for high-precision chronologies to assess recent disturbances on the Great Barrier Reef (GBR), especially the impact of European settlement on reef health, it is important to improve the accuracy of the U/Th dating technique through detailed investigation of local $^{230}Th/^{232}Th_0$ variability. While local estimates of

Table 1
Summary of initial ^{230}Th values obtained from *Porites* corals reported in the literature.

Region	Reef	Lat	Long	Initial $^{230}Th/^{232}Th_{atm}$ ($\times 10^{-6}$)[1]	Initial $^{230}Th/^{232}Th_{act}$[a]	Reference
Taiwan	Nanwan Bay	21°55′N	120°47′E	5.05 ± 1.09	0.94 ± 0.20	Shen et al. (2008)
Vietnam	Son Tra Island	16°13′N	108°12′E	3.20 ± 0.32	0.59 ± 0.06	Shen et al. (2008)
Sumatra	Lewak	02°56′N	95°48′E	3.01 ± 0.47	0.56 ± 0.09	Shen et al. (2008)
	Gusong Bay	02°23′N	96°20′E	7.35 ± 0.65	1.36 ± 0.12	
	Lago	00°03′N	94°32′E	9.4 ± 1.2	1.74 ± 0.22	
	North Pagai	02°35′S	100°06′E	4.7 ± 1.0	0.87 ± 0.19	
	Bulasat	03°07′S	100°19′E	4.9 ± 1.4	0.91 ± 0.26	
	South Pagai	03°07′S	100°19′E	5.02 ± 0.65	0.93 ± 0.12	
Espiritu Santo Is	Malo Is	15°42′S	167°12′E	5.62 ± 2.05 (23.8 ± 4.7)[b]	1.04 ± 0.38 (4.41 ± 0.87)[b]	Shen et al. (2008)
South China Sea	Yongshu Reef	09°32′S	112°52′E	6.81 ± 0.973	1.26 ± 0.18	Yu et al. (2006)
	Meji Reef	09°55′N	115°32′E	7.13 ± 0.324	1.32 ± 0.06	Yu et al. (2006)
Central Pacific	Palmyra Is	05°52′N	162°05′W	20.0	3.70	Cobb et al. (2003a,b)
Great Barrier Reef	Britomart Reef	18°16′S	146°38′E	6.48 ± 3.78	1.2 ± 0.7	McCulloch and Mortimer (2008)
	South Molle Is	20°27′S	148°83′E	5.4	1.00	Zhao et al. (2009a,b)

[a] Where needed, activity values (and atomic values) were calculated using λ_{232} decay constants from Zhang (2008) and λ_{230} decay constants from Cheng et al. (2000).
[b] Denotes anomalously high $^{230}Th/^{232}Th$ value attributed to upwelling of ^{230}Th enriched waters during a La Niña event.

$^{230}Th/^{232}Th_0$ in *Porites* have been determined (McCulloch and Mortimer, 2008; Zhao et al., 2009a), no broad scale, long-term studies have been performed on the near shore reefs of the GBR to assess whether there is any spatial and temporal variability of $^{230}Th/^{232}Th_0$.

On the GBR, distinct water quality gradients are evident both latitudinally and across the continental shelf (Furnas, 2003; Devlin and Brodie, 2005), which may result in large spatial variation in $^{230}Th/^{232}Th_0$ incorporated into the coral skeleton and ultimately influence the accuracy of U-series ages. Modelling of sediment yield from river catchments to the GBR lagoon suggests that following land use intensification (c.1850), the greatest increase in sediment delivery to the GBR occurred in the heavily modified wet–dry catchments in the southern GBR (Neil et al., 2002), while catchments north of 14°S remained relatively unmodified (Furnas, 2003; Brodie and Mitchell, 2005). Furthermore, sclerochronological evidence of a 5–10-fold increase in sediment delivery to the GBR lagoon from 1870 onwards adjacent to modified catchment areas (McCulloch et al., 2003) may also be reflected in a possible long term decline in $^{230}Th/^{232}Th_0$ towards terrestrially derived values.

In this study, thermal ionisation mass spectrometry (TIMS) U-series dating is used to assess the spatial and temporal variability of $^{230}Th_0$ present in living *Porites* coral skeletons of known age sampled over broad spatial scales from the near shore region of the GBR. Such knowledge will further refine the precision and accuracy of the U-series dating method and ultimately increase the temporal resolution for palaeoecological studies.

2. MATERIALS AND METHODS

2.1. Study area

Massive *Porites* coral cores and whole live colonies were sampled from three distinct regions of the GBR that have been subject to varying degrees of land modification in nearby catchment areas. Subsamples from each colony were subsequently used to determine the spatial variation of $^{230}Th_0$ (Table 2).

2.1.1. Far northern Great Barrier Reef

The GBR adjacent to the Cape York Peninsula receives relatively little terrigenous sediment, most of which comes from un-perturbed catchment areas (Woolfe et al., 1998; McKergow et al., 2005; Fig. 1). Although not as well studied as their southern counterparts, rivers in this region are relatively small and exhibit seasonal discharge associated with the Australian summer monsoon (Lough, 1991, 1994; Lambeck and Woolfe, 2000). Catchment areas draining northeast Cape York are estimated to account for ~1–2.5×10^6 tonnes of sediment delivered annually to near shore reefs, which equates to only 7% of the sediment delivery to the GBR lagoon (Neil and Yu, 1996; Woolfe et al., 1998; Furnas, 2003). Flood plumes from the northern rivers are capable of travelling several tens of kilometres offshore (Wolanski, 1994), but by that distance generally contain only low concentrations of suspended sediment (Neil et al., 2002). Sediments are redistributed longshore by wind and wave driven currents to form narrow wedges that extend seawards for less than 5 km, with higher concentrations of terrigenous materials close to the river mouths (Woolfe et al., 1998; Lambeck and Woolfe, 2000). Living *Porites* colonies collected in July 1990 from Eel Reef, Rocky Island and Night Island in the far northern GBR were selected from the Australian Institute of Marine Science (AIMS) core library for this study (Fig. 1; Table 1).

2.1.2. Central Great Barrier Reef

The Palm Islands region lies adjacent to one of the largest and heavily modified catchment areas, the Burdekin River drainage basin. Since European settlement (~1850s) extensive amounts of land has been cleared for agricultural

Table 2
Sample descriptions for living *Porites* coral cores and whole colonies, including collection date, location, total sample length, distance from where the sample was collected with respect to the coastline and nearest influential river.

Region	Reef	Colony	Collection date	Lat S	Long E	Total length (cm)	Distance from coastline (km)	Nearest influential river (km)
Lockhart River (Far northern GBR)	Eel Reef	EelB03S2 EelB07S2 38	Jul 1990	12°30′	143°31′	42 38	18	Pascoe R. (18 km)
	Rocky Is	RocB06S2 RocB07S2	Jul 1990	12°36′	143°24′	28 32	<1	Pascoe R. (18 km)
	Night Is	NigB10S2	Jul 1990	13°10′	143°34′	29	6	Nesbit R. (39 km)
Townsville (Central GBR)	Orpheus Is	OrpB01S1	May 2008			16	16	Herbert R. (20 km); Burdekin R. (164 km)
	Havannah Is	HavB01S2	May 2008	18°50′	146°32′	46 3.5	23	Herbert R. (42 km); Burdekin R. (143 km)
	Pandora Reef	PanB47S2	Aug 2000	18°48′	146°25′	40 4	16	Herbert R. (35 km); Burdekin R. (153 km)
Mackay (Southern GBR)	Round Top Is	RTI	Mar 2006	21°10′	149°15′	86	5	Pioneer R. (5 km)
	Keswick Is	KIB	Apr 2004	20°55′	149°25′	42	26	Pioneer R. (32 km)
		KIC	Apr 2004	20°55′	149°25′	56	26	Pioneer R. (32 km)

purposes, resulting in a 5–10-fold increase in sediments delivered to the Palm Islands (McCulloch et al., 2003; Lewis et al., 2007). River discharge is episodic and seasonal (Belperio, 1983; Moss et al., 1992), occurring during the austral summer months between November and May. Annual sediment delivery to near shore waters at the mouth of the Burdekin is highly variable and estimated to be around 2.7×10^6 (Moss et al., 1992) to 9.0×10^6 (Neil and Yu, 1996) tonnes, with the flood plume capable of extending hundreds of kilometres north (Wolanski and Jones, 1981; King et al., 2002). Examination of various coral proxies in *Porites* from Magnetic Island, Havannah Island and Pandora Reef revealed that these reefs are episodically influenced by flood waters from the Burdekin, Herbert and other smaller tributaries adjacent to the region (Lough et al., 2002; Alibert et al., 2003; McCulloch et al., 2003; Lewis et al., 2007). The Palm Islands region also lies adjacent to the outer boundary of a terrigenous sediment wedge, where periods of high wind and wave activity result in turbid conditions caused by the re-suspension of fine sediments on the inner shelf (Larcombe and Woolfe, 1999). A whole live colony (PanB47S2) was sampled from Pandora Reef by AIMS in August 2000. In May 2008, one core each was collected from a modern *Porites* colonies from the leeward side of both Orpheus and Havannah Island (Fig. 1, Table 1).

2.1.3. Southern Great Barrier Reef

Catchment areas adjacent to the Cumberland Islands in the southern GBR have been cleared primarily for sugarcane cultivation, resulting in large amounts of sediment and fertilizer being transported downstream into the lagoon. Annual sediment loading from the Pioneer-O'Connell River system to the GBR lagoon following catchment disturbance is estimated to be $\sim 0.5 \times 10^6$ tonnes (Neil and Yu, 1996). An examination of Ba/Ca ratios and luminescence in *Porites* skeletons, both proxies for exposure to terrestrial discharge, suggest that flood waters from the Pioneer and Proserpine River are able to extend east as far as Scawfell Island, 51 km offshore (Jupiter et al., 2008). Large tidal ranges of up to 10 m also contribute to unusually high turbidity levels caused by the re-suspension of bottom sediments (Kleypas, 1996). *Porites* cores KIB and KIC from Keswick Island and core RTI from Round Top Island were collected in April 2004 and March 2006, respectively (Fig. 1; Table 1).

2.2. Sample preparation

A total of 11 modern *Porites* samples were sectioned down the main growth axis and a 7 mm thick slice prepared. X-rays of each slab were taken at the University of Queensland Veterinary Clinic. Once annual banding patterns were well constrained in modern *Porites* samples, a 1–2 g sample was drilled from within a single growth band using a bench drill with a 5 mm drill bit. This was repeated three to four times along the length of the colony for different annual growth bands. All samples were then ultrasonically cleaned in deionised water 3–4 times until no visible contaminants were evident and dried at 40 °C on a hotplate under contamination-free conditions (Shen et al., 2008).

2.3. Growth band age determination

The age of each growth band was determined by counting the number of high and low density banding couplets corresponding to one year of growth from the surface of the colony where the year of deposition was known (Lough and Barnes, 1990).

Contributions to the uncertainty of the age of the coral growth bands are well known (Lough and Barnes, 1990, 1992) and are similar to those described for visual-stratigraphic dating of ice cores. Sources of error include sampling resolution, imperfect core stratigraphy and observer bias which ultimately contributes to the misinterpretation of the annual layer record (Alley et al., 1997).

Fig. 1. Map of the Great Barrier Reef (GBR) showing the locations of where each *Porites* sample was taken.

2.3.1. Sampling resolution

In a number of cores, annual growth bands were very narrow (~0.5 cm wide); equalling the same dimensions of the bit used to drill samples. Although great care was taken to ensure samples were taken from the centre of a well constrained growth layer (e.g. 2005.5 AD), the sampling resolution used may span a maximum time period of ±0.5 years; thus a period ranging between, e.g. 2005 and 2006.

2.3.2. Uncertainty in layer counting

Where growth bands were clear in the X-ray images, the true age of each growth band was considered to be accurately identified and a ±0.5 year sampling error (described above) assigned to the age of the density band (Table 2; Fig. 2). Where annual layers were ambiguous, the number of potential annual layers in an unclear section of the colony was determined by dividing the length of section by the average width (~1 cm) of adjacent clearly identifiable bands.

Uncertain annual layers are a major contributor to the total uncertainty of the sample band-counting age. In this study, each uncertain layer was counted as 0.5 ± 0.5 year (see Rasmussen et al., 2006). In the RTI core (Fig. 2), the growth layers prior to the 2000 AD growth band were unclear. This area of the core may represent two indistinguishable bands, one of which we were certain represented

1 year + (0.5 ± 0.5 years) = 1.5 ± 0.5 years. Thus the age of the next clearly identifiable band would be 1998.5 ± 0.5.

The accumulated error obtained by summing up the uncertain annual layers is called the maximum counting error (MCE) and has been used to determine appropriate chronologies in ice cores (Rasmussen et al., 2006). For n uncertain layers it amounts to $n \times 0.5$ years. This calculation was applied in our study to determine the uncertainty of the sample age. Again using the RTI core as an example (Fig. 2), sample RTI-B came from a growth band below two areas of the core where the growth layers were unclear. The number of potential layers in these sections was considered to be six, three of which we were certain exist. Thus, the MCE would be $3 \times 0.5 = 1.5$ years. The age of the RTI-B sample would, therefore, be 1988 ± 1.5. Including sampling error, the total error assigned to the age of the sample would be MCE + 0.5 years, i.e. 1988 ± 2 years.

2.4. U-series chemistry and analytical procedures

Forty-three sub-samples from 11 living *Porites* coral colonies were prepared for U–Th dating using a VG-Sector-54 WARP-filtered high-abundance-sensitivity thermal ionisation mass spectrometer (TIMS) at the Radiogenic Isotope Facility (RIF), University of Queensland, following the analytical protocol described in detail in Zhao et al. (2001, 2009b) and Yu et al. (2006). In this study, each sub-sample weighing ~0.6–~1.3 g was spiked with a ^{229}Th–^{233}U–^{236}U mixed tracer and dissolved in double-distilled nitric acid. After complete digestion, 3–4 drops of H_2O_2 were added, the sample beakers tightly closed and placed on a hot plate at 90 °C overnight to decompose any trace amounts of organic matter and to ensure complete tracer–sample mixing. The sample solution became clear and colourless after full decomposition of organics. They were then evaporated to incipient dryness on the hotplate with the sample beakers shielded from each other using glass tubes (taller and wider in diameter than the beakers) to avoid cross contamination. After standard Fe hydroxide co-precipitation to pre-concentrate U and Th, the insoluble hydroxides were redissolved in 0.2 ml 7 M double-distilled HNO_3 and purified using standard ion-exchange methods (Edwards et al. 1987). U and Th fractions were loaded separately onto single filaments made of zone-refined rhenium ribbons (manufactured by H. Cross Company in the USA) and sandwiched into two graphite layers (about 1 μl of colloidal graphite was used for each layer). Prior to sample loading, the filaments were degassed first at 4.5A for 30 min and then at 5.4 A for another 30 min in a filament outgasser. Th isotopic ratios $^{232}Th/^{229}Th$ and $^{229}Th/^{230}Th$ were measured manually, whereas $^{233}U/^{235}U$, $^{234}U/^{235}U$ and $^{233}U/^{236}U$ were measured automatically on the Daly ion counter of the TIMS in peak-jumping mode. Typical running temperatures are 1750–1850 °C for U and 1900–2100 °C for Th (with $^{232}Th/^{229}Th$ being measured at lower temperature than $^{229}Th/^{230}Th$).

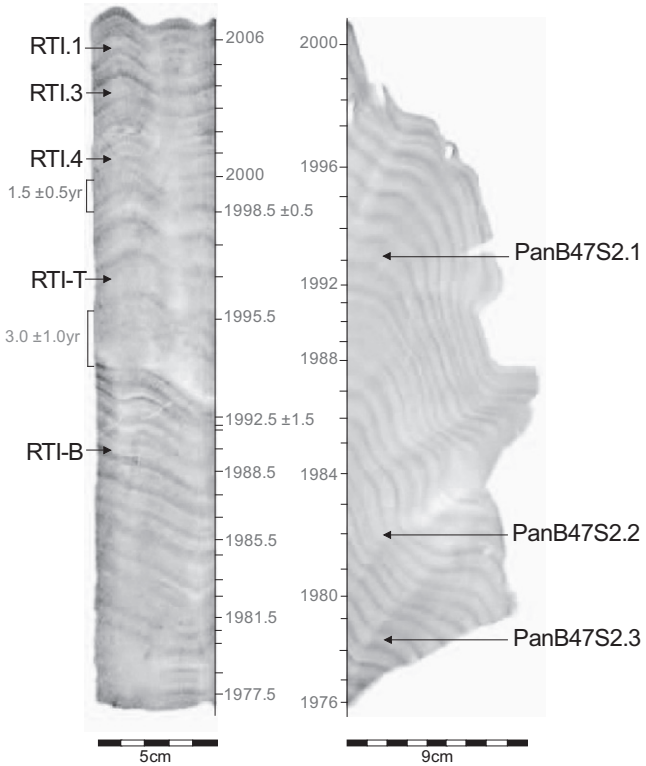

Fig. 2. Positive X-ray image of *Porites* core RTI collected from Round Top Island, southern GBR, where high and low density bands are unclear (left). In this example, the age of each density band couplet was determined by adding together the uncertainty of the age of the previous density bands. Colony PanB47S2 from Pandora Reef, central GBR, where annual density banding patterns are clear (right).

The U isotopic ratios were corrected for mass fractionation by normalising to $^{233}U/^{236}U = 0.96341$ in the spike (see Yu et al., 2006). These ratios, together with the sample and mixed tracer weights, were used to calculate $^{230}Th/^{238}U$ and $^{234}U/^{238}U$ activity ratios as well as U and Th concentrations. Uncorrected ^{230}Th ages were then calculated using Isoplot/Ex 3.00 Programme (Ludwig, 2003). Decay constants used are those reported by Cheng et al. (2000). When measuring the samples in this study, the typical ^{230}Th ion beam intensity was around 5–20 counts per second (cps); 25–100 times higher than the half-mass-unit background (~0.2 cps, which is actually the dark noise level of the Daly detector in this 18-year-old instrument). Signal sizes for all other isotopes were much higher. The operating abundance sensitivity of the TIMS measured at one mass distance on the lower mass side of a large isotope (e.g. ^{238}U, ^{232}Th) in the mass range of U and Th is less than 70 ppb, suggesting that the tailing effect on ^{230}Th from ^{232}Th is negligible.

2.4.1. Spike and standard measurements

During routine U-series dating of carbonate samples on the TIMS in our laboratory, an international uraninite standard HU-1 was frequently measured to monitor the instrument conditions and analytical reproducibility. Long-term repeated measurements of $^{234}U/^{238}U$ atomic ratios in the HU-1 standard yielded a mean value of 54.888 ± 0.050 (2σ, $N = 26$), which is identical to the analytical uncertainty obtained by Cheng et al. (2000). These HU-1 $^{234}U/^{238}U$ measurements were performed by different lab users after spiking the HU-1 standard together with their own batches of unknown samples (usually 20–40 samples in one batch) using the same mixed ^{229}Th–^{233}U–^{236}U tracer and the same column chemistry procedures. In the absence of a reliable gravimetrically-made Th standard solution in our laboratory at the time of this study, the $^{229}Th/^{233}U$ ratios in our mixed ^{229}Th–^{233}U–^{236}U tracer were calibrated against the HU-1 standard by assuming it is in secular equilibrium (i.e. $^{230}Th/^{234}U$ activity ratio = 1); an approach similar to that used by Ludwig et al. (1992) and Hellstrom (2003). The uncertainty associated with this secular equilibrium assumption is less than 0.3% (see Cheng et al., 2000), which is insignificant for dating young coral samples such as those in this study. The mixed ^{229}Th–^{233}U–^{236}U tracer #2 designed for dating young samples in our laboratory was used in this study. The isotopic compositions of this mixed tracer were determined to be: $^{233}U/^{236}U = 0.96341 \pm 0.00033$, $^{233}U/^{238}U = 80.2 \pm 1.2$, $^{233}U/^{234}U = 206.90 \pm 0.62$, $^{233}U/^{235}U = 4405 \pm 26$, $^{229}Th/^{232}Th = 8180 \pm 260$, $^{229}Th/^{230}Th = 20{,}910 \pm 210$ (all errors quoted at 2σ). The spike concentrations are: $^{233}U = 0.0334815$ nmol/g, and $^{229}Th = 0.000892316$ nmol/g, which were obtained by first calibrating the ^{233}U concentration against the known concentration of a gravimetrically-made CRM-112A U metal standard solution and then adjusting ^{229}Th concentration against the mean measured $^{230}Th/^{234}U$ ratio in the secular-equilibrium HU-1 standard.

2.4.2. Blank correction

For TIMS measurements of samples with very young ages, one of the main contributors to age error is the procedural blank from sample preparation and the colloidal graphite used to load samples onto filaments. The total procedural ^{230}Th blank which is mainly derived from the chemistry, was determined to be $1.52 \pm 0.31 \times 10^{-9}$ nmol or 0.00035 ± 0.00007 pg ($N = 12$) (comparable to that of Shen et al., 2008); contributing 0.2 to 1 yr to the ^{230}Th ages of the samples depending on the sample weights and U levels in the samples. Blank contributions have been extracted from the calculation of the measured $^{230}Th/^{232}Th$ and $^{230}Th/^{238}U$ ratios and the corresponding uncorrected ^{230}Th ages (Table 3). Procedural blanks for ^{238}U were $0.5–2.0 \times 10^{-5}$ nmol or 1.2–4.8 pg, which is negligible for coral samples containing ~3 ppm U. Procedural blanks for ^{232}Th were higher and more variable, with a mean of $6.25 \pm 3.04 \times 10^{-5}$ nmol or 14.5 ± 7.1 pg ($N = 12$). We attribute this relatively high ^{232}Th blank to the new colloidal graphite used in the lab as recent multi-collector ICP-MS analysis of similar procedural blanks show the total ^{232}Th procedural blank to be >10 times lower (consistently $<0.6 \times 10^{-5}$ nmol or <1.4 pg). We scanned a large number of zone-refined rhenium filaments in our TIMS and found that out-gassing of the filament at 5.4 A for ~5–10 min is capable of complete removal of residual signals in the U-Th mass range, with the signal at mass 232 < 1 cps (See Zhao et al., 2009b). We found that previous reports of residual signals in this mass range in some zone-refined rhenium filaments were either due to specific filament brands used in those laboratories, or more likely due to deposition of a trace amount of Th onto the posts of the filament holders from previous measurements. After completely polishing off the black burn marks on the posts after each use, no residual signals were ever detected during filament scanning in the TIMS. We also monitored the colloidal graphite blank by loading the same amount of colloidal graphite (~2 μl) onto blank filaments and did find ^{232}Th signals. As the amount of colloidal graphite used for loading samples was volumetrically measured to be the same among all samples, the measured mean ^{232}Th procedural blank of $6.25 \pm 3.04 \times 10^{-9}$ nmol or 14.5 ± 7.1 pg ($N = 12$) should be representative of all samples. ^{232}Th blank correction was applied to the samples measured in this study, which made only a minor difference to the measured ^{232}Th in the samples as ^{232}Th was on average 50–100 times higher. Usually as a large amount of graphite was used for loading young coral samples to maximise the ionisation efficiency and increase the duration of the ion beam, which could be another reason for the high ^{232}Th blanks. Nevertheless, the ^{230}Th blank in the graphite is negligible as monitoring of the blank graphite filaments shows that the ion counts on mass 230 are consistently low; indistinguishable from the dark noise of the TIMS, which is ~0.2 cps (Zhao et al., 2009b). This is not unexpected given the graphite is expected to have much a higher $^{232}Th/^{230}Th$ ratio due to its much higher Th/U ratio.

2.5. Initial $^{230}Th/^{232}Th$ calculation

Previous studies have used living corals to resolve $^{230}Th_0$ by calculating the value required to account for the difference between the 'true age' of the coral determined by annual band counting versus the actual U-series age (Cobb

Table 3
Thermal ionisation mass spectrometry (TIMS) ^{230}Th ages for growth bands sampled from living *Porites* colonies collected from near shore reefs of the Great Barrier Reef.

Sample name[a]	Sample weight (g)	U (ppm)	^{232}Th (ppb)	$(^{230}Th/^{232}Th)_{meas}$	$(^{230}Th/^{238}U)$	$\delta^{234}U$[b]	Uncorr. ^{230}Th age (a)	Time of chemistry	Growth band age (AD)[c]	$(^{230}Th/^{232}Th)_0$[d] $\times 10^{-6}$	$(^{230}Th/^{232}Th)_0$[e]
Far Northern GBR											
EelB03S2.1	1.040	2.4457 ± 0.0027	0.367 ± 0.001	5.92 ± 0.12	0.000292 ± 0.000007	141.5 ± 1.5	27.9 ± 0.7	2009.4	1985.5 ± 0.5	4.77 ± 0.99	0.88 ± 0.18
EelB03S2.2	1.136	2.6579 ± 0.0027	0.379 ± 0.001	7.52 ± 0.12	0.000353 ± 0.000007	141.7 ± 1.2	33.8 ± 0.6	2009.4	1979.5 ± 0.5	4.80 ± 1.00	0.89 ± 0.19
EelB03S2.3	1.105	2.6795 ± 0.0029	0.640 ± 0.003	5.69 ± 0.17	0.000447 ± 0.000014	144.2 ± 1.1	42.7 ± 1.3	2009.4	1973.5 ± 0.5	5.05 ± 1.04	0.94 ± 0.19
EelB07S2.2a	0.801	2.4550 ± 0.0023	0.395 ± 0.002	7.47 ± 0.25	0.000395 ± 0.000013	147.9 ± 1.5	37.6 ± 1.3	2009.9	1983.5 ± 1.5	12.5 ± 1.49	2.31 ± 0.28
EelB07S2.2b	0.955	2.4001 ± 0.0041	0.311 ± 0.002	10.4 ± 0.20	0.000444 ± 0.000009	145.1 ± 1.2	42.4 ± 0.8	2010.2	1983.5 ± 1.5	21.5 ± 1.32	3.97 ± 0.24
EelB07S2.3	0.823	2.5241 ± 0.0026	0.434 ± 0.004	6.46 ± 0.17	0.000366 ± 0.000008	145.1 ± 1.7	34.9 ± 0.8	2009.9	1980.5 ± 1.5	5.72 ± 0.97	1.06 ± 0.18
RocB06S2.1	0.801	2.4327 ± 0.0020	0.611 ± 0.002	3.66 ± 0.05	0.000303 ± 0.000005	143.1 ± 1.4	28.9 ± 0.5	2009.4	1988.0 ± 1.0	5.29 ± 2.15	0.98 ± 0.40
RocB06S2.2	0.955	2.5108 ± 0.0021	0.563 ± 0.002	4.43 ± 0.11	0.000327 ± 0.000009	144.0 ± 1.5	31.3 ± 0.9	2009.4	1985.0 ± 1.5	5.41 ± 1.37	1.00 ± 0.25
RocB06S2.3	0.823	2.0935 ± 0.0019	0.454 ± 0.002	4.85 ± 0.12	0.000346 ± 0.000010	146.8 ± 1.3	33.0 ± 0.9	2009.4	1982.0 ± 2.0	4.57 ± 0.86	0.85 ± 0.16
RocB07S1.1	0.598	2.5304 ± 0.0027	0.179 ± 0.001	11.6 ± 0.24	0.000271 ± 0.000006	147.6 ± 1.9	25.8 ± 0.6	2009.9	1986.5 ± 1.0	6.05 ± 1.99	1.12 ± 0.37
RocB07S1.2	0.602	2.5499 ± 0.0023	0.328 ± 0.002	11.7 ± 0.29	0.000494 ± 0.000011	145.0 ± 1.7	47.2 ± 1.1	2009.9	1983.0 ± 0.5	28.0 ± 1.67	5.18 ± 0.31
RocB07S1.3b	0.841	2.5702 ± 0.0043	0.342 ± 0.003	8.48 ± 0.18	0.000372 ± 0.000007	147.2 ± 1.4	35.4 ± 0.7	2010.2	1977.5 ± 1.0	3.51 ± 1.13	0.65 ± 0.21
RocB07S1.3c	0.340	2.5376 ± 0.0011	0.675 ± 0.001	4.60 ± 0.08	0.000404 ± 0.000007	145.8 ± 1.2	38.5 ± 0.7	2010.7	1977.5 ± 1.0	3.56 ± 0.56	0.66 ± 0.10
NigB10S2.1	1.111	2.3258 ± 0.0022	1.398 ± 0.004	2.47 ± 0.08	0.000488 ± 0.000016	143.9 ± 1.2	46.5 ± 1.6	2009.4	1987.5 ± 1.0	7.28 ± 0.48	1.35 ± 0.09
NigB10S2.2a	1.101	2.6804 ± 0.0028	1.420 ± 0.007	2.62 ± 0.22	0.000456 ± 0.000037	147.2 ± 1.2	43.5 ± 3.6	2009.4	1981.5 ± 1.0	5.22 ± 1.21	0.97 ± 0.22
NigB10S2.2b	1.052	2.7572 ± 0.0031	1.301 ± 0.004	2.89 ± 0.07	0.000449 ± 0.000012	142.5 ± 1.5	43.0 ± 1.1	2009.9	1981.5 ± 0.5	5.49 ± 0.46	1.02 ± 0.09
NigB10S2.3	1.124	2.6170 ± 0.0024	1.113 ± 0.002	3.71 ± 0.10	0.000520 ± 0.000015	146.7 ± 1.0	49.5 ± 1.5	2009.4	1973.0 ± 1.0	5.47 ± 0.65	1.01 ± 0.12
Central GBR											
OrpB01S1.1a	0.625	2.5789 ± 0.0018	0.522 ± 0.002	1.43 ± 0.11	0.000095 ± 0.000009	146.0 ± 1.2	9.0 ± 0.8	2009.4	2007.5 ± 1.0	6.25 ± 1.14	1.16 ± 0.21
OrpB01S1.1b	0.673	2.7141 ± 0.0034	0.906 ± 0.002	1.25 ± 0.03	0.000138 ± 0.000005	145.4 ± 1.7	13.1 ± 0.5	2009.9	2007.5 ± 0.5	5.74 ± 0.84	1.06 ± 0.16
OrpB01S1.2a	1.167	2.7356 ± 0.0027	1.448 ± 0.006	1.21 ± 0.04	0.000209 ± 0.000008	145.4 ± 1.2	20.0 ± 0.8	2009.4	2004.0 ± 1.0	4.88 ± 0.72	0.90 ± 0.13
OrpB01S1.2b	0.451	2.7540 ± 0.0036	1.240 ± 0.006	1.30 ± 0.03	0.000193 ± 0.000006	149.2 ± 1.7	18.4 ± 0.6	2009.9	2004.0 ± 1.0	4.95 ± 0.46	0.92 ± 0.09
OrpB01S1.3	1.114	2.7247 ± 0.0028	0.525 ± 0.002	2.57 ± 0.07	0.000163 ± 0.000005	143.8 ± 1.3	15.5 ± 0.5	2009.4	2000.5 ± 1.5	6.09 ± 0.67	1.13 ± 0.12
PanB47S2.1	1.137	2.4403 ± 0.0020	0.697 ± 0.004	2.54 ± 0.16	0.000238 ± 0.000015	145.5 ± 1.2	22.7 ± 1.5	2009.4	1993.5 ± 0.5	4.23 ± 1.10	0.78 ± 0.20
PanB47S2.2	0.814	2.4238 ± 0.0019	1.271 ± 0.004	2.79 ± 0.05	0.000480 ± 0.000009	146.9 ± 1.2	45.7 ± 0.9	2009.4	1984.5 ± 0.5	7.05 ± 0.45	1.31 ± 0.08
PanB47S2.3	1.254	2.5807 ± 0.0025	0.975 ± 0.003	3.50 ± 0.07	0.000434 ± 0.000009	144.2 ± 1.4	41.4 ± 0.9	2009.4	1979.5 ± 1.0	5.41 ± 0.48	1.00 ± 0.09
HavB01S2.1a	0.704	2.4727 ± 0.0026	0.638 ± 0.002	1.70 ± 0.06	0.000144 ± 0.000007	147.2 ± 1.8	13.7 ± 0.6	2009.4	2005.0 ± 0.5	6.38 ± 1.12	1.18 ± 0.21
HavB01S2.1b	1.224	2.5867 ± 0.0032	1.883 ± 0.014	1.23 ± 0.03	0.000294 ± 0.000007	146.1 ± 1.7	28.0 ± 0.7	2009.9	2005.5 ± 0.5	5.79 ± 0.40	1.07 ± 0.07
HavB01S2.2	1.020	2.5295 ± 0.0026	0.736 ± 0.004	2.05 ± 0.04	0.000196 ± 0.000005	142.8 ± 1.4	18.7 ± 0.5	2009.4	2000.5 ± 0.5	5.97 ± 0.95	1.11 ± 0.18
HavB01S2.3	1.044	2.5201 ± 0.0023	0.606 ± 0.002	3.37 ± 0.09	0.000266 ± 0.000008	142.5 ± 1.2	25.4 ± 0.7	2009.4	1995.0 ± 2.5	8.12 ± 0.92	1.50 ± 0.17
Southern GBR											
KIB.1	1.095	2.3942 ± 0.0028	0.362 ± 0.001	2.74 ± 0.13	0.000136 ± 0.000008	145.7 ± 1.5	13.0 ± 0.8	2009.2	2002.5 ± 0.5	7.54 ± 1.49	1.40 ± 0.28
KIB.2	1.027	2.4781 ± 0.0023	0.336 ± 0.002	3.71 ± 0.13	0.000165 ± 0.000006	145.1 ± 1.4	15.7 ± 0.6	2009.2	1999.5 ± 0.5	8.09 ± 1.54	1.50 ± 0.29
KIB.3	1.226	2.4735 ± 0.0021	0.351 ± 0.001	4.64 ± 0.12	0.000216 ± 0.000007	146.1 ± 1.3	20.6 ± 0.7	2009.2	1996.5 ± 0.5	10.0 ± 1.04	1.86 ± 0.19
KIB.4	0.823	2.2377 ± 0.0022	0.353 ± 0.002	2.58 ± 0.08	0.000134 ± 0.000006	141.3 ± 1.4	12.8 ± 0.5	2010.0	2003.5 ± 0.5	7.28 ± 0.82	1.35 ± 0.15
KIB.5	0.903	2.4562 ± 0.0029	0.305 ± 0.002	3.24 ± 0.15	0.000132 ± 0.000007	148.6 ± 1.6	12.6 ± 0.7	2010.0	2001.5 ± 0.5	6.09 ± 3.73	1.13 ± 0.69
KIB.6	0.853	2.7323 ± 0.0030	0.407 ± 0.002	3.57 ± 0.11	0.000175 ± 0.000006	145.8 ± 1.7	16.7 ± 0.6	2010.0	1998.5 ± 0.5	6.39 ± 0.91	1.18 ± 0.17
KIC.1	1.121	2.5475 ± 0.0028	0.353 ± 0.002	2.62 ± 0.10	0.000119 ± 0.000006	146.1 ± 1.3	11.4 ± 0.5	2009.2	2002.5 ± 0.5	6.16 ± 1.45	1.14 ± 0.27
KIC.2	1.135	2.5026 ± 0.0029	0.400 ± 0.002	3.53 ± 0.11	0.000185 ± 0.000007	147.3 ± 1.2	17.6 ± 0.7	2009.2	1997.5 ± 0.5	6.72 ± 1.33	1.25 ± 0.25

KIC.3	1.270	2.4430 ± 0.0028	0.354 ± 0.002	4.33 ± 0.08	0.000205 ± 0.000005	147.2 ± 1.4	19.6 ± 0.5	2009.2	1994.5 ± 0.5	6.16 ± 1.93	1.14 ± 0.36
RTI.1	1.059	2.5745 ± 0.0031	0.757 ± 0.005	1.52 ± 0.06	0.000147 ± 0.000007	146.1 ± 1.4	14.0 ± 0.6	2009.2	2005.5 ± 0.5	6.32 ± 0.49	1.17 ± 0.09
RTI.3	0.698	3.3503 ± 0.0035	1.178 ± 0.004	1.79 ± 0.04	0.000205 ± 0.000006	145.6 ± 1.5	19.5 ± 0.5	2010.0	2003.5 ± 0.5	6.69 ± 0.58	1.24 ± 0.11
RTI.4	0.580	3.3581 ± 0.0060	2.641 ± 0.013	1.16 ± 0.02	0.000296 ± 0.000006	146.2 ± 2.4	28.2 ± 0.6	2010.0	2000.5 ± 0.5	4.28 ± 0.17	0.79 ± 0.03
RT1-T	1.217	2.5380 ± 0.0025	0.765 ± 0.008	2.43 ± 0.13	0.000240 ± 0.000013	148.6 ± 1.3	22.9 ± 1.2	2008.6	1995.5 ± 1.0	5.81 ± 0.77	1.08 ± 0.14
RT1-B	0.914	2.3802 ± 0.0017	0.998 ± 0.013	2.64 ± 0.09	0.000363 ± 0.000010	148.6 ± 1.2	34.6 ± 0.9	2008.6	1987.5 ± 2.0	5.75 ± 0.58	1.06 ± 0.11

Ratios in parentheses are activity ratios calculated from atomic ratios using decay constants of Cheng et al. (2000). All values have been corrected for laboratory procedural blanks. All errors reported as 2σ. Uncorrected ^{230}Th age (a) was calculated using Isoplot/EX 3.0 programme of Ludwig (2003), where a denotes year.

[a] a and b are replicate samples taken from within the same growth band.

[b] $\delta^{234}U = [(^{234}U/^{238}U) - 1] \times 1000$.

[c] Growth band ages are absolute ages reported in calendar years (AD) derived from visual examination of coral X-rays.

[d] The initial $^{230}Th/^{232}Th$ atomic ratio calculated using the revised U-series age equation from Zhao et al. (2009a,b); 2σ relative error (%).

[e] The initial $^{230}Th/^{232}Th$ activity ratio.

et al., 2003b; Yu et al., 2006; McCulloch and Mortimer, 2008; Burgess et al., 2009). Similarly in this study, $^{230}Th/^{232}Th_0$ values were calculated for live coral samples using the absolute band-counting ages of the corals obtained from X-ray images and the modified U-series age equation for young samples (<1000 years old) described by Zhao et al. (2009b):

$$T_0 \approx \left(\frac{1}{\lambda_{230}}\right)\left(\frac{^{230}Th}{^{234}U}\right)_0 \approx \left(\left(\frac{1}{\lambda_{230}}\right)\left(\frac{Th}{U}\right)_0\left(\frac{\lambda_{232}}{\lambda_{238}}\right)\left(\frac{^{230}Th}{^{232}Th}\right)_0\right)\Big/\left(\frac{^{234}U}{^{238}U}\right)_0 \quad (1)$$

where the isotopic ratios in parentheses refer to the activity ratios and subscript 0 denotes 'initial'. T_0 refers to the 'apparent age' which is related to the presence of initial ^{230}Th ($^{230}Th_0$) at the time of carbonate formation. This equation can be rearranged to solve for $^{230}Th/^{232}Th_0$:

$$\left(\frac{^{230}Th}{^{232}Th}\right)_0 = (T_{uncorr} - T_{abs})\left(\frac{^{234}U}{^{238}U}\right)_0\left(\frac{U}{Th}\right)_0\Big/\left(\frac{\lambda_{232}}{\lambda_{230} \times \lambda_{238}}\right) \quad (2)$$

where T_{uncorr} is the uncorrected ^{230}Th age and T_{abs} is the absolute or 'true' age of the sample deduced from band counting, thus $T_0 = T_{uncorr} - T_{abs}$. $(^{234}U/^{238}U)_0$ and $(U/Th)_0$ approximate the measured $(^{234}U/^{238}U)$ and U/Th ratios for young samples such as those analysed in this study. The $^{230}Th/^{232}Th_0$ error associated with the calculation is derived in Electronic annex EA-1.

2.6. Statistical analyses

Differences in $^{230}Th/^{232}Th_0$ between and within each region were determined using a one-way ANOVA. To account for the propagated uncertainties associated with each $^{230}Th/^{232}Th_0$ value, weighted mean $^{230}Th/^{232}Th_0$ values were also calculated for each region and for the entire GBR using the Isoplot/Ex 3.0 programme (Ludwig, 2003). All $^{230}Th/^{232}Th_0$ values were graphed to identify those which did not fall under a normal Gaussian distribution. These values were then removed and analysed using a Shapiro–Wilk test for normality before calculating weighted means. Long-term temporal changes in $^{230}Th/^{232}Th_0$ were determined using a linear regression.

3. RESULTS

3.1. Uranium and thorium in corals

The TIMS U-series isotopic analytical results for the live *Porites* specimens are listed in Table 3. All U-series ages had $\delta^{234}U$ values analytically within error of 146 ± 3‰, which is typical of modern seawater and corals elsewhere (Delanghe et al., 2002; Robinson et al., 2004; Shen et al., 2008; Andersen et al., 2010). Uranium concentrations ranged between 2.09 and 3.36 ppm (40 out of 43 analyses between 2.24 and 2.76 ppm), similar to other modern *Porites* coral samples (Cobb et al., 2003b; Yu et al., 2006; Shen et al., 2008).

Concentrations of ^{232}Th ranged between 0.18 and 2.64 ppb (40 out of 43 analyses between 0.31 and 1.45 ppb), which appear to be site specific. For instance, samples from Eel Reef, Rocky Island and Keswick Island had low ^{232}Th concentrations ranging between 0.15 and 0.91 ppb. Night Island consistently had high ^{232}Th values ranging between 1.05 and 1.42 ppb. Round Top Island had highly variable ^{232}Th values of 0.76–2.64 ppb. Similar to Round Top Island, the remaining sample locations also exhibited relatively large variation in ^{232}Th concentrations.

3.2. Initial ^{230}Th/^{232}Th (^{230}Th/^{232}Th$_0$) values

The analyses of all 41 coral samples revealed their uncorrected ^{230}Th ages to be older than their band counting ages (Table 3, Fig. 3a). For samples NigB10S2.1, PanB47S2.2 and HavB01S2.1b, the uncorrected age was more than 20 years or up to 55% older than the growth band age. ^{230}Th/^{232}Th$_0$ values calculated using Eq. (2) varied between $3.5 \pm 1.1 \times 10^{-6}$ and $2.15 \pm 0.13 \times 10^{-5}$ (Table 2; Fig. 4). The corresponding two-sigma (2σ) standard deviation associated with the ^{230}Th/^{232}Th$_0$ values ranged from 0.17×10^{-6} to 3.73×10^{-6}, which was highly dependent upon the level of ^{232}Th and band-counting age errors. Thirty-six (88% of samples) of the ^{230}Th/^{232}Th$_0$ values obtained were higher than the bulk Earth atomic value of 4.48–4.70 $\times 10^{-6}$ (Taylor and McLennan, 1995; Wedepohl, 1995). However, only samples EelB07S2.2a, EelB07S2.2b, KIB.2, KIB.3, NigB10S2.1 and PanB47S2.2 had ^{230}Th/^{232}Th$_0$ values and associated errors outside the range of the conservative bulk Earth atomic value of $4.3 \pm 2.2 \times 10^{-6}$ (1σ) proposed by Richards and Dorale (2003). The difference between the uncorrected age and the growth band age in each of these samples was 11.1, 15.3, 6.0, 7.9, 24.6 and 20.7 years, respectively, and was found to be substantially larger compared to other samples from the same colony.

3.2.1. Far northern GBR

^{230}Th/^{232}Th$_0$ values derived from five *Porites* colonies in the far northern GBR showed the greatest variability. The ^{230}Th/^{232}Th$_0$ values for Eel Reef ranged between $4.77 \pm 0.99 \times 10^{-6}$ and $2.15 \pm 0.13 \times 10^{-5}$. Coeval subsamples EelB07S2.2a and EelB07S2.2b (i.e. subsamples collected from the same growth band) revealed a large disparity in ^{230}Th/^{232}Th$_0$ values of $1.25 \pm 0.15 \times 10^{-5}$ and $2.15 \pm 0.13 \times 10^{-5}$, respectively. ^{232}Th concentrations were less than 1 ppb for all samples. The lowest ^{230}Th/^{232}Th$_0$ values for this region occurred in the Rocky Island colonies, with values ranging between $3.5 \pm 1.1 \times 10^{-6}$ and $28.0 \pm 1.7 \times 10^{-6}$. The variability observed between growth bands was similar in magnitude to that observed for Eel Reef located ~18 km away. Low ^{232}Th concentrations, less than 1 ppb, were also characteristic of Rocky Island. The least variation in ^{230}Th/^{232}Th$_0$ was seen in the Night Island colony with values ranging between 5.2 ± 1.2 and $7.28 \pm 0.48 \times 10^{-6}$. ^{232}Th was substantially higher in samples from this colony, located more than 70 km south of Eel and Rocky Island, with concentrations ranging between 1.11 and 1.42 ppb.

3.2.2. Central GBR

The Havannah Island colony had ^{230}Th/^{232}Th$_0$ ranging between 5.79 ± 0.40 and $8.12 \pm 0.92 \times 10^{-6}$. ^{230}Th/^{232}Th$_0$ in the Orpheus Island colony ranged between $4.88 \pm 0.72 \times 10^{-6}$ and $6.3 \pm 1.1 \times 10^{-6}$, with consistent values between duplicate analyses of coeval material. The three samples measured from the Pandora Reef colony showed the greatest variability in ^{230}Th/^{232}Th$_0$, with values ranging between 4.2 ± 1.1 and $7.05 \pm 0.45 \times 10^{-6}$. Samples analysed from the Havannah and Orpheus Island colonies showed a trend of decreasing ^{230}Th/^{232}Th$_0$ with increasing ^{232}Th concentrations; implying mixing of a terrestrial component with high ^{232}Th and low ^{230}Th/^{232}Th$_0$. This was in contrast to the Pandora Reef colony, where higher ^{230}Th/^{232}Th$_0$ values corresponded with higher ^{232}Th concentrations. In all colonies, ^{232}Th concentrations varied between 0.52 and 1.88 ppb.

3.2.3. Southern GBR

Round Top Island ^{230}Th/^{232}Th$_0$ values were consistently low (compared to Keswick Island), ranging between 4.28 ± 0.17 and $6.69 \pm 0.58 \times 10^{-6}$. Samples obtained from Keswick Island 26 km from shore showed high ^{230}Th/^{232}Th$_0$ ranging between $6.1 \pm 3.7 \times 10^{-6}$ and $10.0 \pm 1.0 \times 10^{-6}$. ^{232}Th concentrations were low at this site; less than 0.41 ppb.

3.2.4. ^{230}Th/^{232}Th$_0$ variation between regions

A plot of ^{230}Th/^{232}Th$_0$ versus ^{232}Th (ppb) using all data revealed substantial overlap in ^{230}Th/^{232}Th$_0$ when values were grouped according to region (Fig. 4). Results from a one-way ANOVA confirmed that there was no significant difference between regions ($F_{2,42} = 0.769$; $P = 0.470$). In addition, when each region was examined separately, no significant difference was observed between reefs within the far northern ($F_{2,16} = 0.246$; $P = 0.785$), central ($F_{2,11} = 1.299$; $P = 0.319$) and southern GBR ($F_{1,13} = 4.533$; $P = 0.055$). However, Night Island and Rocky Island were clearly different from the other reefs sampled in the northern and southern regions of the GBR, respectively, due to characteristically high ^{232}Th concentrations (Fig. 4).

The weighted mean for each region and for the entire GBR were calculated using Isoplot/EX 3.0 (Ludwig, 2003) and reported in Table 4. The weighted mean ^{230}Th/^{232}Th$_0$ values for the three regions, $5.35 \pm 0.70 \times 10^{-6}$ for the far northern, $5.77 \pm 0.52 \times 10^{-6}$ for the central and $6.05 \pm 0.59 \times 10^{-6}$ for the southern GBR, were consistent with each other. Samples EelB07S2.2a, EelB07S2.2b, RocB07S1.2, HavB01S2.2 and KIB.3 were removed from the calculations as these values were graphically found not to fall under a normal Gaussian distribution. Once removed, results of a Shapiro–Wilk test revealed a normal distribution for all three regions (far northern $P = 0.392$, central $P = 0.907$ and southern GBR $P = 0.575$). The weighted mean ^{230}Th/^{232}Th$_0$ value for all samples collected across the inshore region of the GBR was $5.52 \pm 0.32 \times 10^{-6}$ (2σ) based on 39 of the 43 samples (Fig. 5). Results of a Shapiro–Wilk test revealed a normal distribution ($P = 0.845$) following the removal of samples KIB.3, RocB07S1.2, EelB07S2.2a and EelB07S2.2b (Fig. 5a).

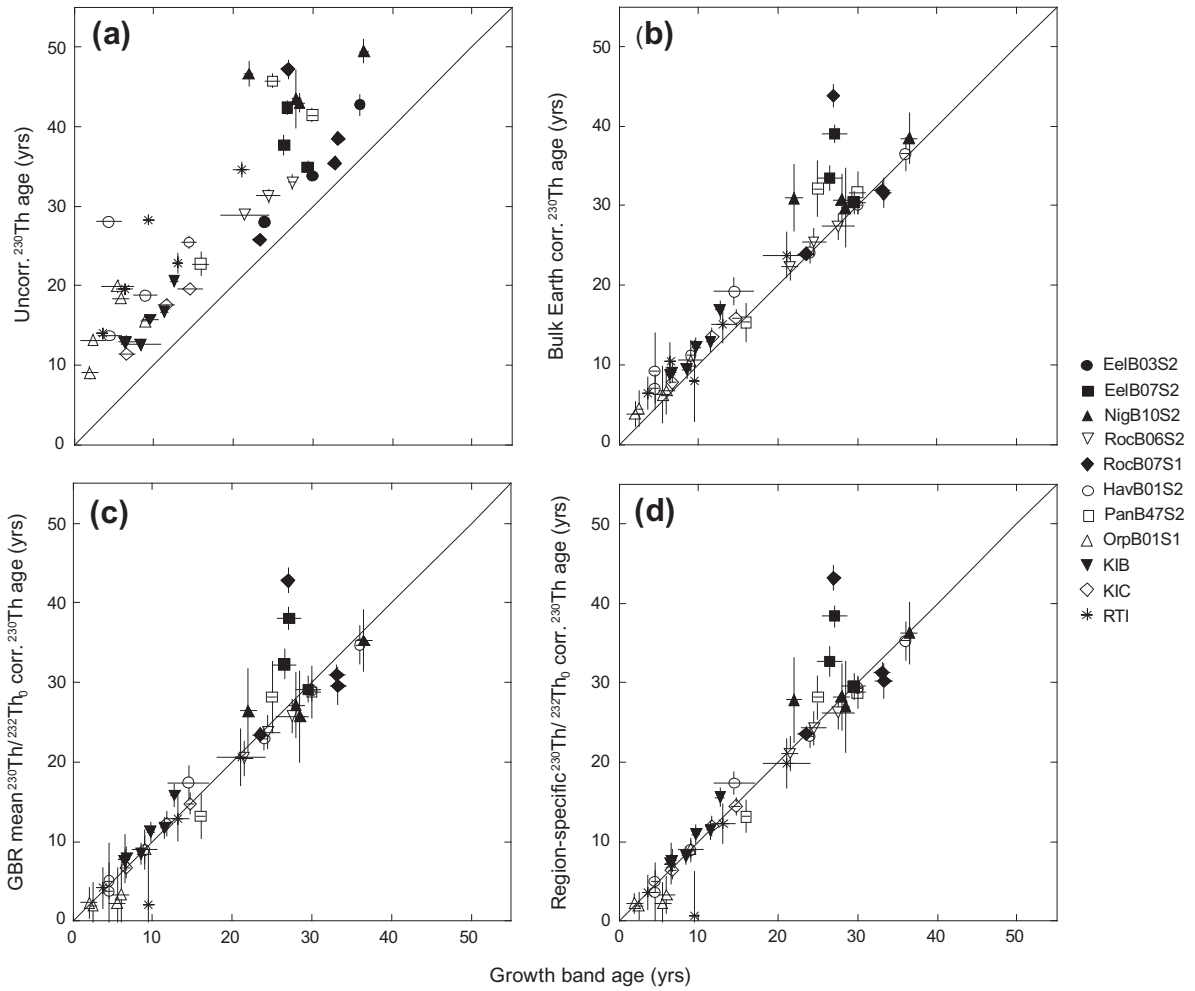

Fig. 3. (a) Uncorrected ^{230}Th age versus growth band age (deduced from coral X-rays) for each sample. Vertical error bars represent analytical error, horizontal error bars represent error associated with band counting. Note that all U-series ages are ~3–25 years older than their 'true' age, indicating substantial amount of $^{230}Th_0$ present in each sample; (b) ^{230}Th age corrected using the bulk Earth atomic $^{230}Th/^{232}Th_0$ value of 4.32×10^{-6} with an assigned uncertainty of 25%; (c) ^{230}Th age corrected using the weighted mean $^{230}Th/^{232}Th_0$ value of 5.52×10^{-6} deduced from 39 *Porites* samples collected along the length of the GBR with an assigned uncertainty of ±25%; (d) ^{230}Th age corrected using the weighted mean $^{230}Th/^{232}Th_0$ value for each region with an assigned uncertainty of ±25% (see Table 4).

It is worth noting that the calculated 2σ errors associated with the weighted means seriously under-estimated the true scatter of the data, as reflected by the large MSWD values for both the region-specific and GBR-wide means (Table 4). By expanding the error ranges to enclose all the data points except the outliers rejected by Isoplot/EX 3.0 programme (i.e. those failing the normal distribution test), the percentage errors for the northern, central, southern GBR regions are 27.1%, 14.6% and 20.3%, respectively, with that for all the 39 data from the entire GBR being 21.2%. Because of this, we assigned a more conservative error of 25% for both region-specific and GBR-wide mean $^{230}Th/^{232}Th_0$ values for calculating the corresponding corrected ^{230}Th ages (see EA-2). Also for comparison, we assigned the same error of 25% for the bulk-Earth $^{230}Th/^{232}Th_0$ value for calculating the corresponding corrected ^{230}Th ages. The corrected ^{230}Th ages based on three different types of $^{230}Th/^{232}Th_0$ values were plotted against the band-counting ages (see Fig. 3). The results indicate that the bulk-Earth-corrected ^{230}Th ages display a general positive bias toward older ages.

3.2.5. Temporal variation in $^{230}Th/^{232}Th_0$

Initial $^{230}Th/^{232}Th$ values were relatively consistent across the entire inshore region of the GBR over a time frame of ~40 years during which the colonies grew (Fig. 6). Results from a Pearson correlation analysis revealed no significant relationship between $^{230}Th/^{232}Th_0$ and growth band age for the far northern ($R^2 = 0.044$, $P = 0.419$), central ($R^2 = -0.042$, $P = 0.705$) and southern region ($R^2 = -0.0039$, $P = 0.833$), suggesting no temporal trend in $^{230}Th/^{232}Th_0$ variability. However, substantial intra-colony variation occurred; for example, colony EelB07S2 exhibited $^{230}Th/^{232}Th_0$ values that differed by close to four times (~27%) among growth bands from $5.72 \pm 0.97 \times 10^{-6}$ to $21.5 \pm 1.3 \times 10^{-6}$. Interestingly, anomalously high $^{230}Th/^{232}Th_0$ values obtained from the EelB07S2 and RocB07S1 colonies appeared to coincide

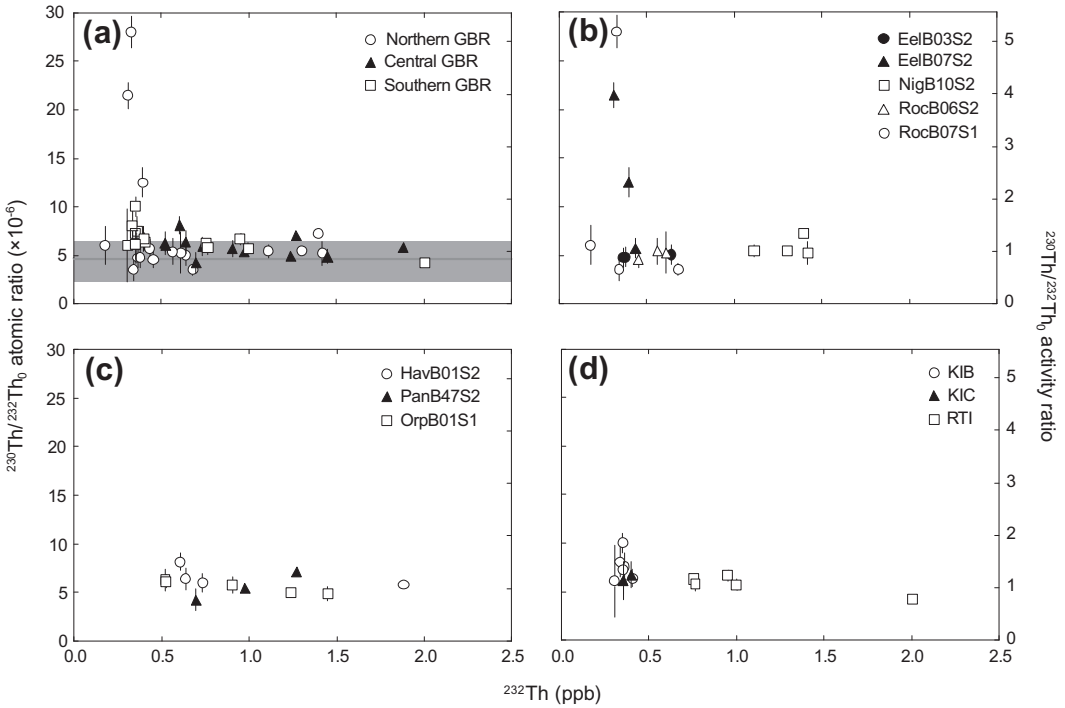

Fig. 4. (a) Broad scale variability of $^{230}Th/^{232}Th_0$ versus ^{232}Th (ppb) for 11 *Porites* colonies sampled from the combined northern, central and southern near shore regions of the GBR. Narrow dark grey line represents the bulk Earth value of $4.48–4.70 \times 10^{-6}$; light grey shading represents conservative bulk Earth value of $4.32 \times 10^{-6} \pm 50\%$. Regions were then divided to show $^{230}Th/^{232}Th_0$ versus ^{232}Th (ppb) variability for the (b) northern; (c) central and; (d) southern GBR.

within the same time period; 1983.5 ± 1.5 and 1983.0 ± 0.5, respectively. It is also worthwhile to note that EelB07S2.2a and EelB07S2.2b represent sub-samples from within the same annual band (1983.5 AD) of the colony. Their $^{230}Th/^{232}Th_0$ values, although varying considerably, are consistently higher than those from other annual bands, suggesting that the anomaly is age specific.

4. DISCUSSION

4.1. Initial $^{230}Th/^{232}Th$ values

U-series analyses of 41 samples from living *Porites* colonies of known age revealed that $^{230}Th/^{232}Th_0$ values for the majority of the samples were higher than the bulk Earth value of $4.48–4.70 \times 10^{-6}$ (Taylor and McLennan, 1995; Wedepohl, 1995), and in most cases higher than values reported in corals from continental shelf sites (Shen et al., 2008). These results, as well as the positive age offsets for most samples corrected using the bulk Earth value (Fig. 3b), suggest that the source of $^{230}Th_0$ incorporated into the coral skeleton during growth is complex. Needless to say, the ^{230}Th ages come close to their respective 'true' ages following correction for $^{230}Th/^{232}Th_0$ using the standard bulk Earth value and could be considered suitable in most cases if the large assigned 50–100% uncertainty is used. However, for extremely young corals, ^{230}Th ages are likely to be under-corrected when the bulk Earth value is used and the large assigned 50–100% uncertainty would result in substantially large age errors (Richards and Dorale, 2003; Cobb et al., 2003b) making it difficult to provide valid interpretations.

Weighted mean $^{230}Th/^{232}Th_0$ for the entire GBR based on the samples collected in this study were normally distributed around a weighted mean value of $5.76 \pm 0.34 \times 10^{-6}$ (with the exception of four possible outliers), which is similar to mean local values obtained by McCulloch and Mortimer (2008) and Zhao et al. (2009a). By expanding the 2-sigma error to 21.2%, the new error range will enclose all 39 data points within their individual 2-sigma error ranges. Thus this mean value with the expanded error, or an even more conservative error of 25% used in Fig. 3, is much more constrained than the conservative bulk Earth value and is a better alternative for $^{230}Th_0$ correction for inshore reef corals in the GBR. Estimates of $^{230}Th/^{232}Th_0$ calculated in this study lie between coastal and open ocean values obtained from *Porites* corals elsewhere (Cobb et al., 2003b; Yu et al., 2006; Shen et al., 2008)(Fig. 7). Initial $^{230}Th/^{232}Th$ values were consistently the highest at Keswick Island, suggesting that either the proportion of terrigenous Th input is less at this site, or the open-ocean $^{230}Th/^{232}Th$ value is anomalously high, or a combination of both. Situated 26 km from shore, this was the farthest sampling location from the mainland. Low $^{230}Th/^{232}Th_0$ values were consistently found in all samples from the Rocky, Orpheus, Havannah and Round Top Island colonies, with values falling within error of the bulk Earth value, or even lower. Rocky and Round Top Island lie

Table 4
Weighted mean $^{230}Th/^{232}Th_0$ activity values for each reef, region and all samples combined.

Region	Reef	Weighted mean $^{230}Th/^{232}Th_0$ ($\times 10^{-6}$)[a]	$\pm 2\sigma$ (95% conf. err; $\times 10^{-6}$)[b]	n	MSWD[d]	p-value[e]	No. rejected	$\pm 2\sigma$ adjusted (%)[c]
Far northern GBR		5.35	0.70	17	9.5	**	3 of 17	27.1
	Eel Reef	7.63	6.22	6	117.7	**	0 of 6	
	Rocky Is	4.08	0.88	7	3.0	*	1 of 7	
	Night Is	6.11	1.61	4	12.3	**	0 of 4	
Central GBR		5.77	0.52	12	6.5	**	1 of 12	14.6
	Orpheus Is	5.36	0.75	5	3.2	*	0 of 5	
	Pandora Reef	6.13	2.93	3	19.0	**	0 of 3	
	Havannah Is	6.16	1.41	4	7.4	**	0 of 4	
Southern GBR		6.05	0.59	14	6.0	**	1 of 14	20.3
	Keswick Is	6.91	0.44	9	1.0	0.42	1 of 9	
	Round Top Is	5.77	1.20	5	11.4	**	0 of 5	
Entire GBR		5.76	0.34	43	8.1	**	4 of 43	21.2

[a] Weighted mean values obtained using Isoplot/EX 3.0 (Ludwig, 2003).
[b] 2σ error for sample RTI.4 increased from 1.73 to 5.4×10^{-6} (see text for details).
[c] 2σ percentage error adjusted to include the full range of $^{230}Th/^{232}Th_0$ values not captured by the weighted mean calculation.
[d] MSWD = Mean Square of Weighted Deviates. The MSWD is the sum of squares of weighted residuals divided by the degrees of freedom. MSWD values greater than unity (i.e. >1) indicate either underestimated analytical errors, or the presence of non-analytical 'geological' scatter (Ludwig, 2003).
[*] p-Value less than 0.05.
[**] p-Value less than 0.01.

within 1 and 5 km of the coastline, respectively. Although Orpheus and Havannah are located further from shore, both islands lie adjacent to a coastal turbid zone and receive sediment laden flood waters from nearby rivers (Larcombe and Woolfe, 1999; McCulloch et al., 2003).

Various researchers have used coral $^{234}U/^{238}U$ measurements and their spatial and temporal variations to source U in seawater (e.g. Andersen et al., 2007; Esat and Yokoyama, 2006, 2010). However, there is no correlation between the measured $^{234}U/^{238}U$ and calculated $^{230}Th/^{232}Th_0$ in our study, probably due to a combination of much lower U concentrations in the riverine waters in the GBR region and the likelihood that $^{234}U/^{238}U$ in the riverine waters (mainly tropical flood waters with very short terrestrial residence time) is not significantly different from the seawater value. Further investigation is needed to clarify if this is the case.

4.2. Spatial and temporal variability

Despite being relatively isolated from anthropogenic activity and having minimal change in sediment delivery since European settlement, $^{230}Th/^{232}Th_0$ values from *Porites* sampled from near shore reefs from the Cape York Peninsula did not vary significantly from values obtained from *Porites* adjacent to highly modified catchment areas (Fig 4a). However, although not significant, the difference in values obtained from Keswick Island and Round Top Island, suggest that a spatial gradient may be present in this region. This is not surprising given that Round Top Island lies within 5 km of the coast and is heavily influenced by tidal re-suspension on a daily basis (Jupiter et al., 2008).

Studies investigating the temporal variation of $^{230}Th/^{232}Th_0$ in carbonates are limited (see Shen et al., 2008). When grouped according to region, initial $^{230}Th/^{232}Th_0$ values have remained relatively constant over the past 20–30 years, with little of the variance explained by time ($r = < 0.1$; $p = > 0.05$ for all three regions). The majority of samples had $^{230}Th/^{232}Th_0$ values that ranged between 3.51 and 8.12×10^{-6} during 1973 ± 1–2007.5 ± 1 AD. Longer records that date back to pre-European settlement may provide better insights into $^{230}Th/^{232}Th_0$ variability and may help to determine whether $^{230}Th/^{232}Th_0$ values have become lower as a result of increased sediment flux to the GBR caused by land clearing and agricultural activity over the past 200 years. Despite the absence of any long-term trends, variability in $^{230}Th/^{232}Th_0$ was observed between growth bands of individual colonies, with values differing by up to four times (e.g. the EelB07S2 colony; Table 2). Interestingly in the far northern GBR, anomalously large $^{230}Th/^{232}Th_0$ values ranging from 12.5 to 28.0×10^{-6} were found to occur within the same time period between 1982 and 1986 AD, despite the locations being 18 km apart.

The spatial and intra-colony variability observed in this study could be attributed to a number of factors including physiological differences between individual colonies as well as local changes in hydrology. Shen et al. (2008) proposed changes in current circulation and upwelling as an explanation for anomalous values obtained from shallow water corals collected from Espiratu Santo Island, Vanuatu. Eel Reef lies adjacent to Cape Weymouth where the continental shelf is at its narrowest (less than 40 km wide compared to approximately 250 km in the south central GBR; Hopley et al., 2007). This area of the GBR is likely to be more influenced by oceanic waters containing high $^{230}Th/^{232}Th_0$ and could explain the large variability in $^{230}Th/^{232}Th_0$ values. A similar explanation could also be given for the consistently high $^{230}Th/^{232}Th_0$ values from Keswick Island. Strong tidal currents passing through the narrow Egremont Passage between Keswick and St. Bees Island (Ayling and

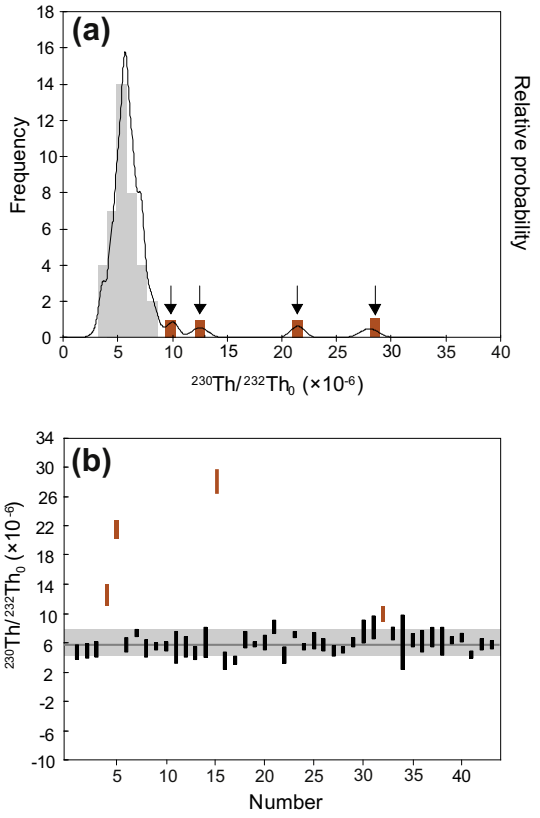

Fig. 5. (a) Cumulative probability plot and histogram of all $^{230}Th/^{232}Th_0$ values. Results of a Shapiro–Wilk test reveal a normal distribution, after excluding four outliers indicated by the arrows. Anomalous values belong to samples RocB07S1.2, EelB07S2.2a, EelB07S2.2b from the northern GBR and KIB.3 from the southern GBR. (b) Plot of all 43 $^{230}Th/^{232}Th_0$ values. The weighted mean of 39 out of 43 values is $5.76 \pm 0.34 \times 10^{-6}$. The shaded area shows an expanded error range to encompass all 39 data points. Bars highlighted in dark grey (or red in the online version) are those values identified as outliers that were subsequently excluded from the calculation. Sample number corresponds to those listed in Table 3. (For interpretation of the references to colour in this figure legend, the reader is referred to the web version of this article.)

Ayling, 2002) where the coral cores were collected, may continuously flush the area with oceanic waters with high dissolved $^{230}Th/^{232}Th_0$.

Temporal variability in $^{230}Th/^{232}Th_0$ in individual cores could also be a result of the high inter-annual variability in precipitation and subsequent changes in water quality. Low values that approach or overlap the bulk Earth value may correspond to flood plumes impacting on the reef during periods of high rainfall or of high wave activity causing the re-suspension of fine particles in the water column. On the other hand, high values may correspond to a period of drought when no major flood events occurred, and river plumes did not reach the reef or during periods of minimal wave activity. In Australia, dry conditions tend to be associated with warm phases of the El Niño-Southern Oscillation (ENSO) or 'El Niño' years, where rainfall and stream flow is consistently below average (Lough, 1994; Chiew et al., 1998; Chiew and McMahon, 2002; Wang and Hendon, 2007). The anomalous values recorded in EelB07S2.2 and RocB07S1 occurred within the 1983 ± 1.5 and 1983 ± 0.5 AD growth layers, which coincide with the 1982–1983 El Niño event (Fig. 8). To a lesser degree, samples NigB10S2.1 from Night Island, HavB01S2.3 from Havannah Is, KIB.3 from Keswick Is, and RTI.3 from Round Top Is also displayed $^{230}Th/^{232}Th_0$ values higher than their site-specific means. Their band-counting ages were 1987.5 ± 1.0, 1995.0 ± 2.5, 1996.5 ± 0.5 and 2003.5 ± 0.5, respectively, matching the 1986–1988, 1994–1995, 1997–1998 and 2002–2003 El Niño events (Fig. 8). During such El Niño -related drier periods, these reefs may have received less terrigenous input. Thus, due to a reduced amount of silts and clays (with high ^{232}Th) entering the GBR lagoon, the high $^{230}Th/^{232}Th$ values may reflect the incorporation of proportionally higher dissolved ^{230}Th produced by the dissolution of carbonate material. Shen et al. (2008) also linked similar anomalies to ENSO extremes. They attributed high $^{230}Th/^{232}Th_0$ values in *Porites* collected from Espiratu Santo Island of Vanuatu in the western Pacific to substantial upwelling of cold water during a strong La Niña episode. However, the influence of ENSO on eastern Australia is not spatially uniform (Rustomji et al., 2009) and the transport of continental dusts (with low $^{230}Th/^{232}Th$) to the GBR lagoon during dry periods (McGowan and Clark, 2008; Marx et al., 2009) may explain why this pattern is not consistent with the rest of the data, highlighting the difficulty in identifying the possible causes for $^{230}Th/^{232}Th_0$ variation.

Local geomorphology may also play a role in the spatial variability of $^{230}Th/^{232}Th_0$. Many of the inshore reefs have developed on terrigenous foundations with much of the reef matrix consisting of terrigenous muddy sand (Hopley et al., 2007). Further from shore, carbonate material becomes the primary reef builder with high $^{230}Th/^{232}Th$. The marked difference (though not significant) in $^{230}Th/^{232}Th_0$ values between Keswick and Round Top Island likely reflects this gradient of increasing $^{230}Th/^{232}Th_0$ with distance from shore.

4.3. Sources of initial ^{230}Th ($^{230}Th_0$) in live *Porites*

The living *Porites* colonies investigated in this study were collected along the near shore region of the GBR, with many of the reefs situated close to or on a terrigenous sediment wedge and regularly exposed to river discharge. Thus, silts and clays transported by nearby rivers are the likely primary source of $^{230}Th_0$ incorporated into the coral skeleton. Corals sampled from these areas should have higher ^{232}Th and lower $^{230}Th/^{232}Th_0$ levels reflecting that of the bulk Earth value. However, $^{230}Th/^{232}Th_0$ varied considerably between low values that reflect coastal settings (Shen et al., 2008) and high values from open ocean environments (Cobb et al., 2003a,b).

Given the setting of this study, it is likely that the dominant source of $^{230}Th_0$ is terrigenous sediment in most cases. ICP-MS measurements of Th/U ratios produced in our laboratory for over 40 dust and river sediment samples from the Burdekin River catchment area give a mean value of 4.8 ± 0.9, corresponding to a mean $^{230}Th/^{232}Th$ atomic

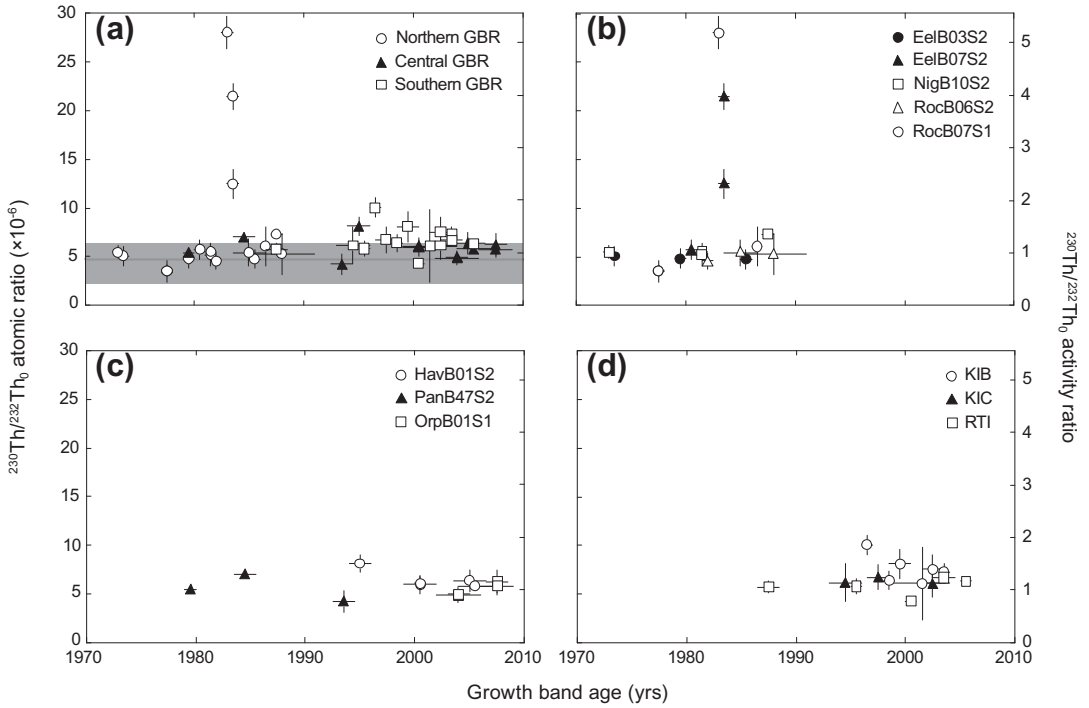

Fig. 6. Temporal variability of $^{230}Th/^{232}Th_0$ measured in live *Porites* colonies from (a) all three regions combined. Narrow dark grey line represents the bulk Earth atomic value of 4.48 to 4.70×10^{-6}; light grey shading represents conservative bulk Earth atomic value of $4.32 \times 10^{-6} \pm 50\%$; (b) far northern ($R^2 = 0.0441$, $P = 0.4185$); (c) central ($R^2 = -0.0420$, $P = 0.7047$); and (d) southern ($R^2 = -0.0039$, $P = 0.8327$) region of the GBR.

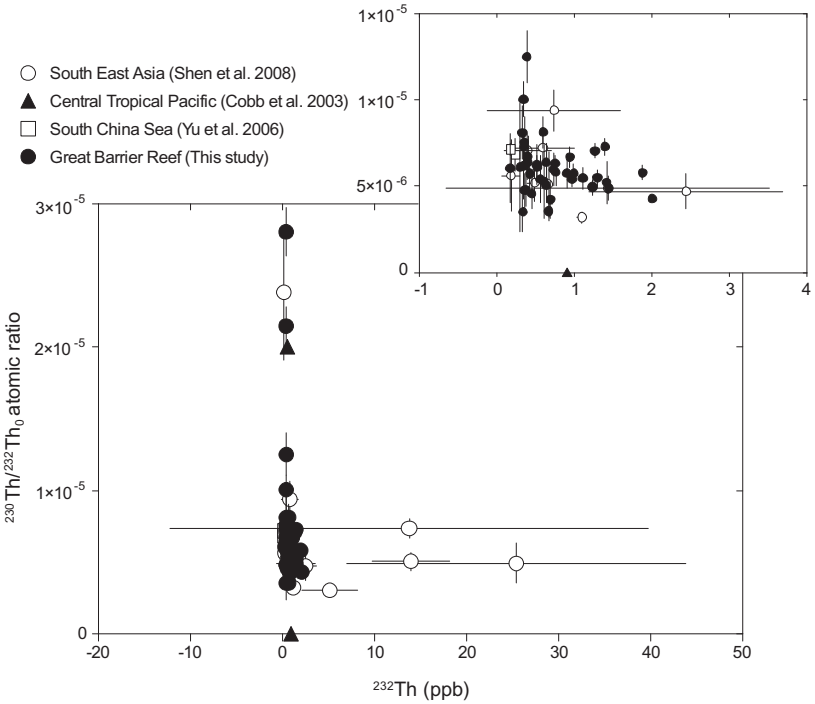

Fig. 7. Comparison of $^{230}Th/^{232}Th_0$ and ^{232}Th from the GBR with published values. Inset is an enlarged image focusing on samples with $^{230}Th/^{232}Th_0$ and ^{232}Th ranging from 0.0 to 1.8 and 0.2 to 3.1, respectively.

ratio of $3.51 \times 10^{-6} \pm 20\%$ (see Cooper et al., 2006).The MUQ (MUd from Queensland) $^{230}Th/^{232}Th$ atomic ratio of $4.05 \times 10^{-6} \pm 20\%$ (corresponding to a mean Th/U ratio of 4.2 ± 0.9) is based on sediment samples taken from 30

rivers in Queensland (Kamber et al., 2005). While these values are within the broad range of the bulk continental crust ratios, their difference highlights the spatial Th/U (or $^{230}Th/^{232}Th$) variability in initial ^{230}Th sources.

The anomalously high, yet short-lived $^{230}Th/^{232}Th_0$ values reported in this study were attributed earlier to strong El Niño events, and suggest that in some instances, a minor but variable contribution of high $^{230}Th/^{232}Th_0$ is accumulated from an alternative source or sources in surrounding waters when terrestrial input is lower than usual. Potential sources of high $^{230}Th/^{232}Th_0$ in such samples, as well as those with $^{230}Th/^{232}Th_0$ values that fall outside the range of local sediment values, are described below.

High $^{230}Th/^{232}Th_0$ values in corals from the central tropical Pacific have been attributed to upwelling deeper waters or carbonate sands (Cobb et al., 2003b). Eel Reef is a large crescentic reef (Hopley et al., 2007), where, when not influenced by the nearby Pascoe River, the carbonate-enriched sandy substrate could be a potential source of ^{230}Th to corals (Robinson et al., 2004). As discussed earlier, the location of Eel Reef on the narrow region of the continental shelf may also expose this area to upwelled waters. For the other reefs with high $^{230}Th/^{232}Th_0$, upwelling from the Coral Sea is generally restricted to outer- and mid-shelf reefs (Andrews and Gentien, 1982; Andrews and Furnas, 1986; Wolanski et al., 1988), and can be ruled out.

High $^{230}Th/^{232}Th_0$ in the water column can also result from the biological dissolution (microboring, macroboring) and grazing of carbonate material. Rates of bioerosion range from <0.5 to 1.81 kg m^{-2} of $CaCO_3$ after 3 years for inshore reefs, and up to 6.07 kg m^{-2} after 3 years in offshore reefs (Tribollet et al., 2002; Tribollet and Golubic, 2005; Aline, 2008). This redistribution of older carbonate material may potentially contribute a significant amount of ^{230}Th to the water column which is then readily available for recycling by other corals.

Hydrogenous thorium adsorbed to detritus is another potential source of high $^{230}Th/^{232}Th_0$, and could be explained in terms of the activity of thorium nuclides in the marine environment as well as the active feeding behaviour of corals. Suspended particulate matter (SPM), including mangrove detritus, are colonised by bacteria and macroalgae (Blum et al., 1988; Simon et al., 2002) and are able to produce acidic polysaccharides and colloidal polysaccharides on their cell surface which have been found to have high binding constants with Th(IV) (Fisher et al., 1987; Hirose and Tanoue, 2001; Quigley et al., 2001). A recent study by Mahmood et al. (2010) found significant correlations between organic carbon and thorium isotopes, suggesting that organic carbon is a ^{230}Th and ^{232}Th scavenger in marine environments. In turbid inshore environments, numerous symbiotic coral species become active heterotrophs, feeding on various forms of SPM as an alternative energy source to photosynthetic carbon (Risk et al., 1994; Anthony, 1999; Anthony and Fabricius, 2000). By measuring $\delta^{13}C$, Risk et al. (1994) determined that terrigenous matter is a significant source of carbon for inshore corals. Thus, high $^{230}Th/^{232}Th$ values may be a result of bacteria adsorbed to mangrove detritus or 'marine snow' preferentially scavenging ^{230}Th over ^{232}Th. Although the pathway of thorium cations into the aragonite lattice is not well defined (Rosenheim et al., 2007), such particles with potentially high $^{230}Th/^{232}Th_0$ may be taken up by the coral as it switches from autotrophy to heterotrophy in turbid conditions and incorporated into the carbonate skeleton. Despite being located more than ~39 km from the nearest influential river, Night Island is a characteristically turbid reef environment with extensive mangrove colonisation on the reef top (Hopley et al., 2007). The anomalously high ^{232}Th and $^{230}Th/^{232}Th_0$ reported here, likely reflects a combination of both terrestrially derived particulates as well as hydrogenous and/or adsorbed $^{230}Th_0$ on detritus. Corals may also switch to heterotrophy following bleaching (Grottoli et al., 2006). This mechanism may provide an alternative explanation for the high $^{230}Th/^{232}Th_0$ values reported during El Niño years. Nevertheless, while the above explanations seem plausible, in order to validate the source of high $^{230}Th/^{232}Th_0$, $^{230}Th/^{232}Th$ values in both seawater and sediment should be analysed for each location (Robinson et al., 2004; Shen et al., 2008).

4.4. Application of local $^{230}Th_0$ values

This study reveals a weighted mean $^{230}Th/^{232}Th_0$ value of $5.76 \pm 0.34 \times 10^{-6}$ (5.90%) for the entire GBR with a high MSWD of 8.1; suggesting a significant scatter in $^{230}Th/^{232}Th_0$ values exists unrelated to internal analytical errors (Table 4). On the other hand, the expanded error of $\pm 1.17 \times 10^{-6}$ (21.2%) encompasses the full variation of 39 out of the 43 $^{230}Th/^{232}Th_0$ values that show a normal

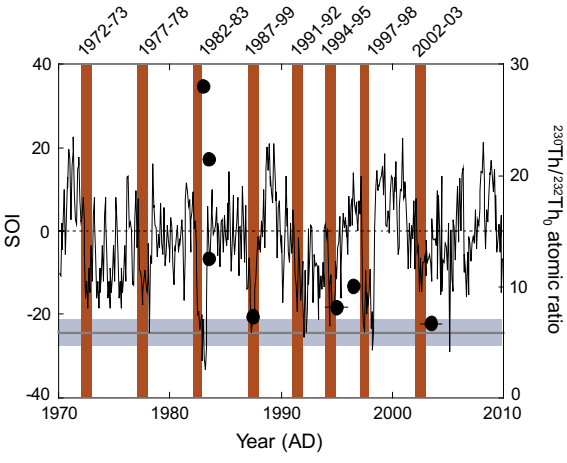

Fig. 8. Monthly Southern Oscillation Index (SOI) starting from January 1970 (source: Australian Bureau of Meteorology) compared with $^{230}Th/^{232}Th_0$ values determined to be above the weighted average for their respective region (black circles). Vertical bars represent El Niño years. Grey shading represents the conservative mean $^{230}Th/^{232}Th_0$ range for the GBR ($5.76 \pm 21.2\%$) that encompasses the 39 data showing normal distribution. Note that the positive $^{230}Th/^{232}Th_0$ anomalies are mostly correlated with El Niño years within their band-counting errors.

Gaussian distribution (Fig. 5). Compared with a 50–100% uncertainty generally assigned to the bulk Earth $^{230}Th/^{232}Th$ correction value, this value is much more constrained. As described in Section 3, a similar approach was also applied to the weighted mean $^{230}Th/^{232}Th_0$ values for each region. To assess the validity of using a GBR-wide and region-specific $^{230}Th/^{232}Th_0$ value for $^{230}Th_0$ correction, we examined the effect these different $^{230}Th/^{232}Th_0$ values for correction would have on the accuracy and precision of each of the ^{230}Th ages when compared to their respective 'true age' (Fig. 3). To ensure each $^{230}Th/^{232}Th_0$ value for correction was equally weighted and corrected ^{230}Th ages are comparable, we assigned the same error (±25%) to each of these ratios. The corrected ^{230}Th age and the corresponding band-counting age fall within error of the 1:1 line in Fig. 3 for most samples regardless of the $^{230}Th/^{232}Th_0$ correction value used for $^{230}Th_0$. However, when compared to the corrected ^{230}Th ages based on the bulk Earth $^{230}Th/^{232}Th_0$ value, most of the corrected ^{230}Th ages based on the GBR-wide and region-specific mean $^{230}Th/^{232}Th_0$ values fall directly on the 1:1 line, closely matching their corresponding band-counting ages (see also EA-2). In contrast, the corrected ^{230}Th ages based on the bulk Earth $^{230}Th/^{232}Th_0$ value are on average significantly older than the band-counting ages, suggesting the use of the bulk Earth value resulted in an overall slight under-correction of the ^{230}Th ages. Since there is little difference between the GBR-wide and region-specific mean $^{230}Th/^{232}Th_0$ values within the assigned 25% error, the GBR-wide mean value would be suitable for the ^{230}Th age corrections in most cases.

When applying the GBR-wide and region-specific mean $^{230}Th/^{232}Th_0$ values for $^{230}Th_0$ correction, the corrected ^{230}Th ages for a few samples differ substantially from their band-counting ages, as shown by those data points lying above or below the 1:1 line in Fig. 3c and d. These samples are either under- or overcorrected for $^{230}Th_0$, respectively. This could be due to the fact that the weighted mean and standard deviation for each region may be based on too few data points that may not encompass the full range of $^{230}Th/^{232}Th_0$ values. Considering that the anomalous $^{230}Th/^{232}Th_0$ values at some sites occurred during El Niño years and subsequently represented short-lived events, duplicate determination of coeval samples, or preferably measurement of different growth bands of known age difference, should be employed to verify the age accuracy (Shen et al., 2008).

In addition, this study also demonstrates that, in cases where age precisions are not the most critical (e.g. for samples of older ages), the use of the bulk-Earth $^{230}Th/^{232}Th_0$ value with a larger assigned error of ±50–100% for initial ^{230}Th correction is applicable to most corals from inshore settings of the GBR.

5. CONCLUSIONS

In the absence of any broad scale data for the GBR region, mean $^{230}Th/^{232}Th_0$ values measured from live *Porites* corals of known age in this study can be used as a reasonable *a priori* estimate of initial ^{230}Th. Such site-specific or region-specific mean $^{230}Th/^{232}Th_0$ values are more appropriate than the bulk-Earth value for $^{230}Th_0$ correction in coral ^{230}Th age calculation. The majority of the $^{230}Th/^{232}Th_0$ values fall within the range of 3.5 ± 1.1–$8.1 \pm 1.1 \times 10^{-6}$ with a weighted mean of $5.76 \pm 0.34 \times 10^{-6}$ (2σ) with a MSWD of 8.1. The mean value is similar to previously reported values from the GBR. However, as the 2σ error of the weighted mean is far too small, we expanded the uncertainty to $\pm 1.17 \times 10^{-6}$ (±21.2%) to encompass the full variation of $^{230}Th/^{232}Th_0$ measurements well beyond their analytical errors. This error is still much smaller than the commonly assigned uncertainty of ±50–100% for the bulk-Earth $^{230}Th/^{232}Th_0$ value used for ^{230}Th age correction. Because of this, we suggest that the weighted mean value of 5.76×10^{-6} with a more conservative assigned error of ±25% be used for ^{230}Th age corrections for most corals from the inshore region of the GBR, provided the samples do not contain a significant amount of terrestrial sediment nor anomalously high $^{230}Th/^{232}Th_0$. Considering the large variability in $^{230}Th/^{232}Th_0$, especially the short-lived anomalous values associated with El Niño years, it is also recommended that duplicate analyses of coeval samples or growth bands of known age be used to verify the accuracy of ^{230}Th dating. The results of this study demonstrate that accurate U/Th dating is achievable for pristine corals of <100 years with a precision of ±1–5 years, especially if the MC-ICP-MS analytical technique with substantially higher sample throughput and smaller sample size is used in future studies, which is more feasible for a large number of duplicate analyses. Knowledge of local $^{230}Th/^{232}Th_0$ values will be valuable for improving both the precision and accuracy of U/Th ages obtained from *Porites* corals to temporally constrain not only paleoclimate reconstructions, but also disturbance events. This is particularly important for coastal coral reefs which are under the greatest pressure from anthropogenic disturbance (van Woesik et al., 1999; Fabricius, 2005).

ACKNOWLEDGEMENTS

We acknowledge P. Colls and L. Evans from the University of Queensland Sample Preparation Laboratory for their help with sample preparation. Special thanks to the staff at the Veterinary X-ray clinic (University of Queensland, UQ), G. Roff and C. Reymond for coring *Porites* in the Palm Islands, E. Matson for preparing *Porites* for our use from the AIMS core library, the management staff of Orpheus Island Research Station (OIRS) and members of the UQ Radiogenic Isotope Facility and the UQ Marine Palaeoecology Laboratory for critical discussions. This research is partially funded by a Marine and Tropical Science Research Facility (MTRSF) Project 1.1.4 grant to J. Zhao, J.M. Pandolfi and T. Done, and is also supported by an Australian Postgraduate Award to T.R. Clark.

APPENDIX A. SUPPLEMENTARY DATA

Supplementary data associated with this article can be found, in the online version, at doi:10.1016/j.gca.2011.11.032.

REFERENCES

Abram N. J., Gagan M. K., McCulloch M. T., Chappell J. and Hantoro W. S. (2003) Coral reef death during the 1997 Indian Ocean dipole linked to Indonesian wildfires. *Science* **301**, 952–955.

Alibert C., Kinsley L., Fallon S. J., McCulloch M. T., Berkelmans R. and McAllister F. (2003) Source of trace element variability in Great Barrier Reef flood plumes. *Geochim. Cosmochim. Acta* **67**, 231–246.

Aline T. (2008) Dissolution of dead corals by euendolithic microorganisms across the northern Great Barrier Reef (Australia). *Microb. Ecol.* **55**, 569–580.

Alley R. B., Shuman C. A., Meese D. A., Gow A. J., Taylor K. C., Cuffey K. M., Fitzpatrick J. J., Grootes P. M., Zielinski G. A., Ram M., Spinelli G. and Elder B. (1997) Visual-stratigraphic dating of the GISP2 ice core: basis, reproducibility, and application. *J. Geophys. Res. Oceans* **102**, 26367–26381.

Andersen M. B., Stirling C. H., Porcelli D., Halliday A. N., Andersson P. S. and Baskaran M. (2007) The tracing of riverine U in Arctic seawater with very precise $^{234}U/^{238}U$ measurements. *Earth Planet. Sci. Lett.* **259**, 171–185.

Andersen M. B., Stirling C. H., Zimmerman B. and Halliday A. N. (2010) Precise determination of the open ocean $^{234}U/^{238}U$ composition. *Geochem. Geophys. Geosyst.* **11**, 1525–2027.

Andrews J. C. and Furnas M. J. (1986) Subsurface intrusions of Coral Sea water into the central Great Barrier Reef I. Structures and shelf-scale dynamics. *Cont. Shelf Res.* **6**, 491–514.

Andrews J. C. and Gentien P. (1982) Upwelling as a source of nutrients for the Great Barrier Reef ecosystems: a solution to Darwin's question? *Mar. Ecol. Prog. Ser.* **8**, 257–269.

Anthony K. R. N. (1999) Coral suspension feeding on fine particulate matter. *J. Exp. Mar. Biol. Ecol.* **232**, 85–106.

Anthony K. R. N. and Fabricius K. E. (2000) Shifting roles of heterotrophy and autotrophy in coral energetics under varying turbidity. *J. Exp. Mar. Biol. Ecol.* **252**, 221–253.

Ayling A. M. and Ayling A. L. (2002) Long-term monitoring program for the marine benthos in the vicinity of Keswick Island development (Whitsunday Island group): baseline survey. Great Barrier Reef Marine Park Authority, Townsville.

Belperio A. P. (1983) Terrigenous sedimentation in the central Great Barrier Reef lagoon – A model from the Burdekin region. *BMR J. Aust. Geol. Geophys.* **8**, 179–190.

Bischoff J. L. and Fitzpatrick J. A. (1991) U-series dating of impure carbonates: an isochron technique using total-sample dissolution. *Geochim. Cosmochim. Acta* **55**, 543–554.

Blum L. K., Mills A. L., Zieman J. C. and Zieman R. T. (1988) The abundance of bacteria and fungi in seagrass and mangrove detritus. *Mar. Ecol. Prog. Ser.* **42**, 73–78.

Brodie J. E. and Mitchell A. W. (2005) Nutrients in Australian tropical rivers: changes with agricultural development and implications for receiving environments. *Mar. Freshwater Res.* **56**, 279–302.

Burgess S. N., McCulloch M. T., Mortimer G. E. and Ward T. M. (2009) Structure and growth rates of the high-latitude coral: *Plesiatrea versipora*. *Coral Reefs* **28**, 1005–1015.

Chappell J., Omura A., Esat T., McCulloch M., Pandolfi J., Ota Y. and Pillans B. (1996) Reconciliation of late Quaternary sea levels derived from coral terraces at Huon Peninsula with deep sea oxygen isotope records. *Earth Planet. Sci. Lett.* **141**, 227–236.

Chen J. H., Curran H. A., White B. and Wasserburg G. J. (1991) Precise chronology of the last interglacial period – ^{234}U–^{230}Th data from fossil coral reefs in the Bahamas. *Geol. Soc. Am. Bull.* **103**, 82–97.

Cheng H., Edwards R. L., Hoff J., Gallup C. D., Richards D. A. and Asmerom Y. (2000) The half-lives of uranium-234 and thorium-230. *Chem. Geol.* **169**, 17–33.

Chiew F. H. S. and McMahon T. A. (2002) Global ENSO-streamflow teleconnection, streamflow forecasting and interannual variability. *Hydrol. Sci. J.* **47**, 505–522.

Chiew F. H. S., Piechota T. C., Dracup J. A. and McMahon T. A. (1998) El Nino Southern Oscillation and Australian rainfall, streamflow and drought: links and potential for forecasting. *J. Hydrol.* **204**, 138–149.

Cobb K. M., Charles C. D., Cheng H. and Edwards R. L. (2003a) El Nino/Southern Oscillation and tropical Pacific climate during the last millennium. *Nature* **424**, 271–276.

Cobb K. M., Charles C. D., Cheng H., Kastner M. and Edwards R. L. (2003b) U/Th-dating living and young fossil corals from the central tropical Pacific. *Earth Planet. Sci. Lett.* **210**, 91–103.

Cooper M., Shields G., Faithful J. and Zhao J. (2006) Using Sr/Nd isotopic ratios to determine sediment sources in the Burdekin Falls Dam, Queensland, Australia. *Geochim. Cosmochim. Acta* **70**, A112.

Delanghe D., Bard E. and Hamelin B. (2002) New TIMS constraints on the uranium-238 and uranium-234 in seawaters from the main ocean basins and the Mediterranean Sea. *Mar. Chem.* **80**, 79–93.

Devlin M. J. and Brodie J. (2005) Terrestrial discharge into the Great Barrier Reef Lagoon: nutrient behaviour in coastal waters. *Mar. Pollut. Bull.* **51**, 9–22.

Edwards R. L., Chen J. H. and Wasserburg G. J. (1987) ^{238}U-^{234}U-^{230}Th-^{232}Th systematics and the precise measurement of time over the past 500,000 years. *Earth Planet. Sci. Lett.* **81**, 175–192.

Edwards R. L., Taylor F. W. and Wasserburg G. J. (1988) Dating earthquakes with high-precision thorium-230 ages of very young corals. *Earth Planet. Sci. Lett.* **90**, 371–381.

Eisenhauer A., Wasserburg G. J., Chen J. H., Bonani G., Collins L. B., Zhu Z. R. and Wyrwoll K. H. (1993) Holocene sea-level determination relative to the Australian continent: U/Th (TIMS) and ^{14}C (AMS) dating of coral cores from the Abrolhos Islands. *Earth Planet. Sci. Lett.* **114**, 529–547.

Esat T. M. and Yokoyama Y. (2006) Variability in the uranium isotopic composition of the oceans over glacial–interglacial timescales. *Geochim. Cosmochim. Acta* **70**, 4140–4150.

Esat T. M. and Yokoyama Y. (2010) Coupled uranium isotope and sea-level variations in the oceans. *Geochim. Cosmochim. Acta* **74**, 7008–7020.

Fabricius K. A. (2005) Effects of terrestrial runoff on the ecology of corals and coral reefs: review and synthesis. *Mar. Pollut. Bull.* **50**, 125–146.

Fisher N. S., Teyssie J. L., Krishnaswami S. and Baskaran M. (1987) Accumulation of Th, Pb, U, and Ra in marine-phytoplankton and its geochemical significance. *Limnol. Oceanogr.* **32**, 131–142.

Furnas M. (2003) *Catchments and corals: terrestrial runoff to the Great Barrier Reef*. Australian Institute of Marine Science, Townsville.

Gagan M. K., Ayliffe L. K., Beck J. W., Cole J. E., Druffel E. R. M., Dunbar R. B. and Schrag D. P. (2000) New views of tropical paleoclimates from corals. *Quat. Sci. Rev.* **19**, 45–64.

Grottoli A. G., Rodrigues L. J. and Palardy J. E. (2006) Heterotrophic plasticity and resilience in bleached corals. *Nature* **440**, 1186–1189.

Hellstrom J. (2003) Rapid and accurate U/Th dating using parallel ion-counting multi-collector ICP-MS. *J. Anal. At. Spectrom.* **18**, 1346–1351.

Hirose K. and Tanoue E. (2001) Strong ligands for thorium complexation in marine bacteria. *Mar. Environ. Res.* **51**, 95–112.

Hopley D., Smithers S. G. and Parnell K. E. (2007) *The Geomorphology of the Great Barrier Reef: Development, Diversity, and Change*. Cambridge University Press, Cambridge.

Jupiter S., Roff G., Marion G. S., Henderson M., Schrameyer V., McCulloch M. T. and Hoegh-Guldberg O. (2008) Linkages between coral assemblages and coral proxies of terrestrial exposure along a cross-shelf gradient on the southern Great Barrier Reef. *Coral Reefs* **27**, 887–903.

Kamber B. S., Greig A. and Collerson K. D. (2005) A new estimate for the composition of weathered young upper continental crust from alluvial sediments, Queensland, Australia. *Geochim. Cosmochim. Acta* **69**, 1041–1058.

King B., McAllister F. and Done T. (2002) Modelling the impact of the Burdekin, Herbert, Tully and Johnstone River plumes on the Central Great Barrier Reef. CRC Reef Research Centre Technical Report No. 44. CRC Reef Research Centre, Townsville.

Kleypas J. A. (1996) Coral reef development under naturally turbid conditions: fringing reefs near Broad Sound, Australia. *Coral Reefs* **15**, 153–167.

Lambeck A. and Woolfe K. J. (2000) Composition and textural variability along the 10 m isobath, Great Barrier Reef: evidence for pervasive northward sediment transport. *Aust. J. Earth Sci.* **47**, 327–335.

Larcombe P. and Woolfe K. J. (1999) Terrigenous sediments as influences upon Holocene nearshore coral reefs, central Great Barrier Reef, Australia. *Aust. J. Earth Sci.* **46**, 141–154.

Lewis S. E., Shields G. A., Kamber B. S. and Lough J. M. (2007) A mulit-trace element coral record of land-use changes in the Burdekin River catchment, NE Australia. *Palaeogeogr. Palaeocl.* **246**, 471–487.

Lough J. M. (1991) Rainfall variations in Queensland, Australia – 1891–1986. *Int. J. Climatol.* **11**, 745–768.

Lough J. M. (1994) Climate variation and El Niño Southern Oscillation events on the Great Barrier Reef – 1958 to 1987. *Coral Reefs* **13**, 181–195.

Lough J. M. and Barnes D. J. (1990) Intra-annual timing of density band formation of *Porites* coral from the central Great Barrier Reef. *J. Exp. Mar. Biol. Ecol.* **135**, 35–57.

Lough J. M. and Barnes D. J. (1992) Comparisons of skeletal density variations in *Porites* from the central Great Barrier Reef. *J. Exp. Mar. Biol. Ecol.* **155**, 1–25.

Lough J. M., Barnes D. J. and McAllister F. A. (2002) Luminescent lines in corals from the Great Barrier Reef provide spatial and temporal records of reefs affected by land runoff. *Coral Reefs* **21**, 333–343.

Ludwig K. R. (2003) *Users Manual for Isoplot/Ex version 3.0: A Geochronological Toolkit for Microsoft Excel*. Berkeley Geochronology Centre, Berkeley.

Ludwig K. R., Simmons K. R., Szabo B. J., Winograd I. J., Landwehr J. M., Riggs A. C. and Hoffman R. J. (1992) Mass-spectrometric Th-230-U-234-U-238 dating of the Devils Hole calcite vein. *Science* **258**, 284–287.

Lybolt M., Neil D. T., Zhao J.-X., Feng Y.-X., Yu F.-F. and Pandolfi J. (2010) Instability in marginal coral reef: the shift from natural variability to a human-dominated seascape. *Front. Ecol. Environ.*, doi:10.1890/090176.

Mahmood Z. U. W., Ahmad Z., Adziz M. I. A., Mohamed C. A. R. and Ishak A. K. (2010) Radioactivity distribution of thorium in sediment core of the Sabah-Sarawak coast. *J. Radioanal. Nucl. Chem.* **285**, 365–372.

Marx S. K., McGowan H. A. and Kamber B. S. (2009) Long-range dust transport from eastern Australia: a proxy for Holocene aridity and ENSO-type climate variability. *Earth Planet. Sci. Lett.* **282**, 167–177.

McCulloch M. T. and Mortimer G. E. (2008) Applications of the ^{238}U–^{230}Th decay series to dating of fossil and modern corals using MC-ICPMS. *Aust. J. Earth Sci.* **55**, 955–965.

McCulloch M. T., Fallon S. J., Wyndham T., Hendy E. J., Lough J. M. and Barnes D. J. (2003) Coral record of increased sediment flux to the inner Great Barrier Reef since European settlement. *Nature* **421**, 727–730.

McGowan H. and Clark A. (2008) Identification of dust transport pathways from Lake Eyre, Australia using Hysplit. *Atmos. Environ.* **42**, 6915–6925.

McKergow L. A., Prosser I. P., Hughes A. O. and Brodie J. (2005) Sources of sediment to the Great Barrier Reef world heritage area. *Mar. Pollut. Bull.* **51**, 200–211.

Moss A. J., Rayment G. E., Reilly N. and Best E. K. (1992) *A preliminary assessment of sediment and nutrient exports from Queensland coastal catchments. Queensland Department of Environment and Heritage Technical Report No. 5*. Queensland Department of Environment and Heritage, Brisbane.

Natawidjaja D. H., Sieh K., Ward S. N., Cheng H., Edwards R. L., Galetzka J. and Suwargadi B. W. (2004) Paleogeodetic records of seismic and aseismic subduction from central Sumatran microatolls, Indonesia. *J. Geophys. Res.* **109**. doi:10.1029/2003JB002398.

Neil D. T. and Yu B. (1996) Fluvial sediment yield to the Great Barrier Reef Lagoon: spatial patterns and the effect of land use. In *Downstream Effects of Land Use* (eds. H. M. Hunter, A. G. Eyles and G. E. Rayment). Department of Natural Resources, Brisbane, pp. 281–286.

Neil D. T., Orpin A. R., Ridd P. V. and Yu B. (2002) Sediment yield and impacts from river catchments to the Great Barrier Reef lagoon. *Mar. Freshwater Res.* **53**, 733–752.

Pandolfi J. M., Bradbury R. H., Sala E., Hughes T. P., Bjorndal K. A., Cooke R. G., McArdle D., McClenachan L., Newman M. J. H., Paredes G., Warner R. R. and Jackson J. B. C. (2003) Global trajectories of the long-term decline of coral reef ecosystems. *Science* **301**, 955–958.

Quigley M. S., Santschi P. H., Guo L. D. and Honeyman B. D. (2001) Sorption irreversibility and coagulation behavior of Th-234 with marine organic matter. *Mar. Chem.* **76**, 27–45.

Rasmussen S. O., Andersen K. K., Svensson A. M., Steffensen J. P., Vinther B. M., Clausen H. B., Siggaard-Andersen M. L., Johnsen S. J., Larsen L. B., Dahl-Jensen D., Bigler M., Röthlisberger R., Fischer H., Goto-Azuma K., Hansson M. E. and Ruth U. (2006) A new Greenland ice core chronology for the last glacial termination. *J. Geophys. Res.* **111**. doi:10.1029/2005JD006079.

Richards D. A. and Dorale J. A. (2003) Uranium-series chronology and environmental applications of speleothems. In *Uranium-Series Geochemistry*, vol. 52 (eds. B. Bourdon, G. M. Henderson, C. C. Lundstrom and S. P. Turner). Mineralogical Society of America, Washington, DC, pp. 407–460.

Risk M. J., Sammarco P. W. and Schwarcz H. P. (1994) Cross-continental shelf trends in $\delta^{13}C$ in coral on the Great Barrier Reef. *Mar. Ecol. Prog. Ser.* **106**, 121–130.

Robinson L. F., Belshaw N. S. and Henderson G. M. (2004) U and Th concentrations and isotope ratios in modern carbonates and waters from the Bahamas. *Geochim. Cosmochim. Acta* **68**, 1777–1789.

Rosenheim B. E., Swart P. K. and Eisenhauer A. (2007) Constraining initial Th-230 activity in incrementally deposited, biogenic aragonite from the Bahamas. *Geochim. Cosmochim. Acta* **71**, 4025–4035.

Rustomji P., Bennett N. and Chiew F. (2009) Flood variability east of Australia's Great Dividing Range. *J. Hydrol.* **374**, 196–208.

Shen C., Li K., Sieh K., Natawidjaja D. H., Cheng H., Wang X., Edwards R. L., Lam D. D., Hsieh Y., Fan T., Meltzner A. J., Taylor F. W., Quinn T. M., Chiang H. and Kilbourne K. H. (2008) Variation of initial $^{230}Th/^{232}Th$ and limits of high precision U–Th dating of shallow water corals. *Geochim. Cosmochim. Acta* **72**, 4201–4223.

Sieh K., Natawidjaja D. H., Meltzner A. J., Shen C., Cheng H., Li K., Suwargadi B. W., Galetzka J., Philibosian B. and Edwards R. L. (2008) Earthquake supercycles inferred from sea-level changes recorded in the corals of western Sumatra. *Science* **322**, 1674–1678.

Simon M., Grossart H. P., Schweitzer B. and Ploug H. (2002) Microbial ecology of organic aggregates in aquatic ecosystems. *Aquat. Microb. Ecol.* **28**, 175–211.

Stein M., Wasserburg G. J., Lajoie K. R. and Chen J. H. (1991) U-series ages of solitary corals from the California coast by mass spectrometry. *Geochim. Cosmochim. Acta* **55**, 3709–3722.

Stirling C. H., Esat T. M., Lambeck K., McCulloch M. T., Blake S. G., Lee D. C. and Halliday A. N. (2001) Orbital forcing of the marine isotope stage 9 interglacial. *Science* **291**, 290–293.

Taylor S. R. and McLennan S. M. (1995) The geochemical evolution of the continental-crust. *Rev. Geophys.* **33**, 241–265.

Tribollet A. and Golubic S. (2005) Cross-shelf differences in the pattern and pace of bioerosion of experimental carbonate substrates exposed for 3 years on the northern Great Barrier Reef, Australia. *Coral Reefs* **24**, 422–434.

Tribollet A., Decherf G., Hutchings P. A. and Peyrot-Clausade M. (2002) Large-scale spatial variability in bioerosion of experimental coral substrates on the Great Barrier Reef (Australia): importance of microborers. *Coral Reefs* **21**, 424–432.

van Woesik R., Tomascik T. and Blake S. (1999) Coral assemblages and physico-chemical characteristics of the Whitsunday Islands: evidence of recent community changes. *Mar. Freshwater Res.* **50**, 427–440.

Wang G. and Hendon H. H. (2007) Sensitivity of Australian rainfall to inter-El Nino variations. *J. Climate* **20**, 4211–4226.

Wedepohl K. H. (1995) The composition of the continental crust. *Geochim. Cosmochim. Acta* **59**, 1217–1232.

Wolanski E. (1994) *Physical Oceanographic Processes of the Great Barrier Reef*. CRC Press, Boca Raton.

Wolanski E. and Jones M. (1981) Physical properties of Great Barrier Reef Lagoon waters near Townsville. I. Effects of Burdekin River floods. *Aust. J. Mar. Fresh. Res.* **32**, 305–319.

Wolanski E., Drew E., Abel K. M. and Obrien J. (1988) Tidal jets, nutrient upwelling and their influence on the productivity of the alga *Halimeda* in the Ribbon Reefs, Great Barrier Reef. *Estuar. Coast Shelf S.* **26**, 169–201.

Woolfe K. J., Larcombe P., Orpin A. R., Purdon R. G., Michaelsen P., McIntyre C. M. and Amjad N. (1998) Controls upon inner-shelf sedimentation, Cape York Peninsula, in the region of 12°S. *Aust. J. Earth Sci.* **45**, 611–621.

Yu K. F., Zhao J. X., Shi Q., Chen T. G., Wang P. X., Collerson K. D. and Liu T. S. (2006) U-series dating of dead *Porites* corals in the South China Sea: evidence for episodic coral mortality over the past two centuries. *Quat. Geochronol.* **1**, 129–141.

Yu K. F., Zhao J. X., Shi Q. and Meng Q. S. (2009b) Reconstruction of storm/tsunami records over the last 4000 years using transported coral blocks and lagoon sediments in the southern South China Sea. *Quat. Int.* **195**, 128–137.

Zachariasen J., Sieh K., Taylor F. W., Edwards R. L. and Hantoro W. S. (1999) Submergence and uplift associated with the giant 1833 Sumatran subduction earthquake: evidence from coral microatolls. *J. Geophys. Res.* **104**, 895–919.

Zhang Y. (2008) *Geochemical kinetics*. Princeton University Press, Princeton.

Zhao J. X., Hu K., Collerson K. D. and Xu H. K. (2001) Thermal ionisation mass spectrometry U-series dating of a hominid site near Nanjing, China. *Geology* **29**, 27–30.

Zhao J. X., Neil D. T., Feng Y. X., Yu K. F. and Pandolfi J. M. (2009a) High-precision U-series dating of very young cyclone-transported coral reef blocks from Heron and Wistari reefs, southern Great Barrier Reef, Australia. *Quat. Int.* **195**, 122–127.

Zhao J. X., Yu K. F. and Feng Y. X. (2009b) High-precision ^{238}U–^{234}U–^{230}Th disequilibrium dating of the recent past – A review. *Quat. Geochronol.* **4**, 423–433.

Associate editor: Yuri Amelin